IEEE Access
Multidisciplinary | Rapid Review | Open Access Journal

Received October 18, 2019, accepted November 2, 2019, date of publication November 7, 2019, date of current version November 20, 2019.

Digital Object Identifier 10.1109/ACCESS.2019.2952293

Joint Subcarrier Assignment and Global Energy-Efficient Power Allocation for Energy-Harvesting Two-Tier Downlink NOMA Hetnets

MOHAMMED W. BAIDAS[1], (Senior Member, IEEE), MUBARAK AL-MUBARAK[2], (Student Member, IEEE), EMAD ALSUSA[3], (Senior Member, IEEE), AND MOHAMAD KHATTAR AWAD[4], (Senior Member, IEEE)

[1]Department of Electrical Engineering, College of Engineering and Petroleum, Kuwait University, Kuwait City 13060, Kuwait
[2]Department of Electrical and Computer Engineering, The Ohio State University, Columbus, OH 43210, USA
[3]School of Electrical and Electronic Engineering, The University of Manchester, Manchester M13 9PL, U.K.
[4]Department of Computer Engineering, College of Engineering and Petroleum, Kuwait University, Kuwait City 13060, Kuwait

Corresponding author: Mohammed W. Baidas (m.baidas@ku.edu.kw)

This work was supported in part by the Kuwait Foundation for the Advancement of Sciences (KFAS), under Project Code PN17-15EE-02, in part by the European Union's Horizon 2020 Research and Innovation Programme, under Grant No. 812991, and in part by the Kuwait University Research Grant No. EO-08/18.

ABSTRACT In this paper, the problem of joint subcarrier assignment and global energy-efficient power allocation (J-SA-GEE-PA) for energy-harvesting (EH) two-tier downlink non-orthogonal multiple-access (NOMA) heterogeneous networks (HetNets) is considered. Particularly, the HetNet consists of a macro base-station (MBS) and a number of small base-stations (SBSs), which are solely powered via renewable-energy sources. The aim is to solve the J-SA-GEE-PA maximization problem subject to quality-of-service (QoS) per user as well as other practical constraints. However, the formulated J-SA-GEE-PA problem happens to be non-convex and NP-hard, and thus is computationally-prohibitive. In turn, problem J-SA-GEE-PA is split into two sub-problems: (1) subcarrier assignment via many-to-many matching, and (2) GEE-maximizing power allocation. In the first sub-problem, the subcarriers are assigned to users via the Gale-Shapley deferred acceptance mechanism. As for the second sub-problem, the GEE-PA problem is solved optimally via a low-complexity algorithm. After that, a two-stage solution procedure is devised to efficiently solve the J-SA-GEE-PA problem, while ensuring stability. Simulation results are presented to validate the proposed solution procedure, where it is shown to efficiently yield comparable network global energy-efficiency to the J-SA-GEE-PA scheme, and superior to that of OFDMA; however, with lower computational-complexity. The algorithmic designs presented in this work constitute a step towards filling the gap for computationally-efficient and effective resource allocation solutions to guarantee a fully autonomous and grid-independent operation of EH two-tier downlink NOMA HetNets.

INDEX TERMS Energy-efficiency, heterogeneous networks, matching, non-orthogonal multiple-access, power allocation, subcarrier assignment.

I. INTRODUCTION

The ever increasing demand for massive connectivity, spectral- and energy-efficiency, low latency, and higher throughput—while meeting quality-of-service (QoS) requirements for cellular users—have become motivating factors for designing effective resource allocation solutions for fifth-generation (5G) cellular networks and beyond. To meet such pressing demands, heterogeneous networks (HetNets) have been proposed as a means for network

The associate editor coordinating the review of this manuscript and approving it for publication was Wei Wang.

densification, so as to improve cellular coverage, capacity and spectrum utilization [1], [2]. However, conventional orthogonal multiple-access (OMA) schemes—when utilized in HetNets—do not adequately utilize spectrum resources to meet the demands of future generation cellular networks. In turn, non-orthogonal multiple-access (NOMA) has been proposed to further improve spectrum utilization and capacity [3]. Particularly, in NOMA, multiple users are multiplexed in the power-domain by exploiting channel gains' differences and imbalanced power allocation, while utilizing successive interference cancellation (SIC) for multiuser detection [4]. Despite the numerous advantages of NOMA, if power allocation is not carefully optimized, severe interference may be introduced to neighbouring cells within the HetNet architecture, leading to severe performance degradation. On the other hand, the fast growing energy consumption and limited energy resources have further pushed the need for energy-efficient transmission schemes [5]. Moreover, due to the scarcity of the energy resources, energy-harvesting (EH) has emerged as a potential technology and viable solution to energize cellular networks via renewable energy sources, ultimately reducing dependency on the electrical grid [6]. However, harvested energy is based on random and intermittent energy arrivals, and thus fixed energy supply cannot be guaranteed or predicted in advance [7]. Hence, there is an urgent need for optimal and energy-efficient transmission schemes to improve the network energy-efficiency and reliability in EH NOMA-enabled HetNets, while satisfying QoS requirements.

Recently, several research works have considered resource allocation in NOMA HetNets. For instance, the tradeoff between energy-efficiency (EE) and spectral-efficiency (SE) in downlink NOMA HetNets is studied in [8]. Particularly, the tradeoff is formulated as a multi-objective optimization problem (MOP), subject to maximum transmit power and minimum rate requirements. The MOP is then transformed into a single-objective optimization problem, and the joint sub-channel allocation and power allocation problem is solved via an iterative algorithm. It has been shown that the proposed algorithm is superior to the orthogonal frequency-division multiple-access (OFDMA)-based scheme. In [9], network throughput maximization in downlink NOMA HetNets is considered, where the problem proves to be NP-hard. Thus, the authors propose a scheduling scheme and an iterative distributed power control algorithm, which have been shown to be superior to OMA HetNets and single-tier NOMA networks in terms of spectral efficiency, and outage performance. In [10], the authors study the tradeoff among energy efficiency, fairness, harvested energy, and sum-rate in NOMA-based HetNets. Specifically, various fairness metrics and two SIC ordering approaches are considered. In turn, joint subcarrier and power allocation algorithms are proposed for each fairness metric and SIC ordering approach. In particular, an iterative algorithm utilizing successive convex approximation is employed to solve the power allocation problem, while the mesh adaptive direct search algorithm is used to solve the subcarrier assignment problem. In [11], a distributed user formation and resource allocation framework for imperfect NOMA HetNets is proposed, where receiver sensitivity and interference residue from non-ideal SIC are characterized. Additionally, the effects of fractional error factor levels, cluster bandwidth, and QoS user demands on the NOMA cluster size are investigated. Then, a clustering algorithm and a distributed $\alpha-$fair resource allocation framework are devised to achieve a tradeoff between maximum throughput and proportional-fairness. In [12], the authors study the problem of joint user association and power control (J-UA-PC) for energy-efficiency maximization in two-tier downlink NOMA HetNets. Particularly, the base-stations are powered by renewable energy sources as well the conventional grid. In addition, energy-cooperation among the base-stations has been incorporated via the smart grid. In turn, a distributed algorithm for optimal user association—for fixed power allocation—is proposed based on the Lagrangian dual analysis. Then, a J-UA-PC algorithm is devised to further maximize the energy-efficiency, which has also been shown to outperform OMA-based networks. Joint energy-efficient subchannel and power allocation in downlink NOMA HetNets is studied in [13], where the formulated problem takes the form of mixed-integer non-convex optimization. Hence, convex relaxation and dual decomposition techniques are utilized to optimize subchannel and power allocation by alternatively optimizing the macro-cell and small-cells' resource allocation. It has been demonstrated that the proposed resource allocation scheme attains higher energy-efficiency than that of the OMA scheme.

In this paper, the problem of joint subcarrier assignment and global energy-efficient power allocation (J-SA-GEE-PA) for EH two-tier downlink NOMA HetNets is studied. In particular, the HetNet consists of a macro base-station (MBS) and a number of small base-stations (SBSs), which are solely powered via renewable-energy sources. Specifically, the aim is to solve the joint subcarrier assignment and global energy-efficiency problem; subject to various constraints, such as QoS per user, number of users per subcarrier, number of subcarriers assignable to each user, SIC decoding order, and energy availability. However, the formulated J-SA-GEE-PA maximization problem happens to be non-convex and NP-hard, and thus is computationally-prohibitive [14]. In turn, problem J-SA-GEE-PA is split into two sub-problems: (1) subcarrier assignment via many-to-many matching, and (2) GEE-maximizing power allocation. The first sub-problem is modeled as a two-sided many-to-many matching problem, and solved via the Gale-Shapley deferred acceptance (DA) mechanism [15]. In particular, a polynomial-time complexity algorithm is devised based on the DA mechanism, where the users aim to be assigned to subcarriers that maximize their rates, while the subcarriers' goal is to be assigned to users which minimize the energy consumption. As for the second sub-problem, the global energy-efficient power allocation is solved optimally via a low-complexity

algorithm, while incorporating both intra-cell and/or inter-cell interferences. After that, a two-stage solution procedure is devised to solve the J-SA-GEE-PA problem by first performing subcarrier assignment and GEE-maximizing power allocation for the MBS-tier, and then the subcarrier assignment in the SBS-tier, followed by network GEE-maximizing power allocation, while ensuring two-sided exchange-stability via a polynomial-time complexity swap matching algorithm [16]. Simulation results are presented to validate the efficacy of the proposed solution procedure, which will be shown to efficiently yield comparable network global energy-efficiency to the J-SA-GEE-PA scheme (solved via a global optimization package), and superior to that of OFDMA; however, with lower computational-complexity.

To the best of the authors' knowledge, no prior work has considered joint subcarrier assignment and global energy-efficient power allocation for EH two-tier downlink NOMA HetNets, and provided a computationally-efficient two-stage solution procedure. Thus, the main contributions of this work can be summarized as follows:

- Formulated the problem of joint subcarrier assignment and global energy-efficient power allocation for EH two-tier downlink NOMA HetNets, subject to QoS constraints as well as other practical constraints.
- Modeled the problem of subcarrier assignment as a two-sided many-to-many matching problem, and solved it via the DA algorithm, and within polynomial-time complexity.
- Proposed a low-complexity algorithm to optimally solve the GEE-maximizing power allocation problem, with proven convergence and optimality.
- Devised a two-stage solution procedure to solve the J-SA-GEE-PA problem, which solves the subcarrier assignment and GEE-maximizing power allocation problem in the MBS- and SBS-tiers, while guaranteeing two-sided exchange-stability via a polynomial-time complexity swap matching algorithm.
- Evaluated the proposed two-stage solution procedure, which is shown to efficiently yield comparable network global energy-efficiency to the J-SA-GEE-PA scheme, and superior to that of OFDMA; however, with lower computational-complexity.

Our work differs from [12] from several perspectives. Particularly, no electrical grid or energy-cooperation among the base-stations is considered, as our network model is solely based on renewable-energy sources, where the harvested energy is random and cannot be predicted in advance. In addition, our network model assumes a number of subcarriers rather than a single frequency band shared by all the users in the network. Furthermore, the work in [12] solves the users association problem, while our network model assumes fixed user association prior to the network operation; however, multiple subcarriers may be assigned to each user, and each subcarrier may be assigned to multiple users. On the other hand, the work in [13] assumes that each small-cell can occupy one subchannel, and small-cells can reuse the same subchannel, while the macro-cell can transmit over all subchannels. Moreover, the network power supply is assumed to be fixed and available throughout the network operation. Also, inter-cell interference between small-cells is neglected, which is not the case in our work. Furthermore, the energy-efficient resource allocation is decoupled into two problems, one for small-cells, and the other for the macro-cell; whereas in our work, the subcarrier assignment is decoupled from the global energy-efficient power allocation, and are performed over two stages in the MBS- and SBS-tiers. In summary, the algorithmic designs presented in this work are novel and aim at filling the gap for efficient and effective resource allocation solutions to guarantee a fully autonomous and grid-independent operation for EH two-tier downlink NOMA HetNets.

The rest of this paper is organized as follows. In Section II, the system model is presented, while Section III presents the joint subcarrier assignment and global energy-efficient power allocation problem formulation. Section IV models the subcarrier assignment as a many-to-many matching problem, while Section V presents the algorithmic solutions of the global energy-efficiency maximizing power allocation. Section VI presents the swap matching algorithm, while Section VII outlines the proposed two-stage solution procedure for the joint subcarrier assignment and global energy-efficient power allocation problem. Section VIII presents the simulation results, whereas Section IX draws the conclusions.

II. SYSTEM MODEL

A. NETWORK MODEL

Consider a two-tier downlink HetNet consisting of a macro base-station (MBS) and M small base-stations (SBSs), where the downlink transmission is achieved via NOMA. Let the set of all base-stations in the network be denoted $\mathcal{B} = \{BS_0, BS_1, \ldots, BS_m, \ldots, BS_M\}$, where BS_0 is the MBS, while BS_m (for $m = 1, 2, \ldots, M$) refers to the m^{th} SBS. The frequency spectrum is divided into a set of K orthogonal subcarriers, denoted $\mathcal{SC} = \{SC_1, \ldots, SC_k, \ldots, SC_K\}$, where SC_k is the k^{th} subcarrier. Additionally, let $\mathcal{U} = \{\mathcal{U}_0, \ldots, \mathcal{U}_M\}$ be the set of all N users in the network, where $\mathcal{U}_0$ is the subset of users associated with the MBS (i.e. BS_0), while $\mathcal{U}_m$ is the subset of users associated with SBS BS_m. In particular, the user subsets $\mathcal{U}_0, \ldots, \mathcal{U}_m, \ldots, \mathcal{U}_M$ partition $\mathcal{U}$. That is, $\mathcal{U}_m \cap \mathcal{U}_{m'} = \emptyset$ for $m \neq m'$, and $\bigcup_{m=0}^{M} \mathcal{U}_m = \mathcal{U}$, where $|\mathcal{U}| = N$. The channel between any base-station BS_m and user $U_i \in \mathcal{U}_m$ over subcarrier SC_k is assumed to follow narrowband Rayleigh fading with zero-mean N_0-variance additive white Gaussian noise (AWGN). Specifically, let $h_{m,i}^{k} \sim \mathcal{CN}\left(0, d_{m,i}^{-\nu}\right)$ be a complex Gaussian random variable with zero-mean and variance $d_{m,i}^{-\nu}$, where $d_{m,i}$ is the corresponding distance, while ν is the path-loss exponent. Furthermore, perfect channel state information is assumed at the base-stations.

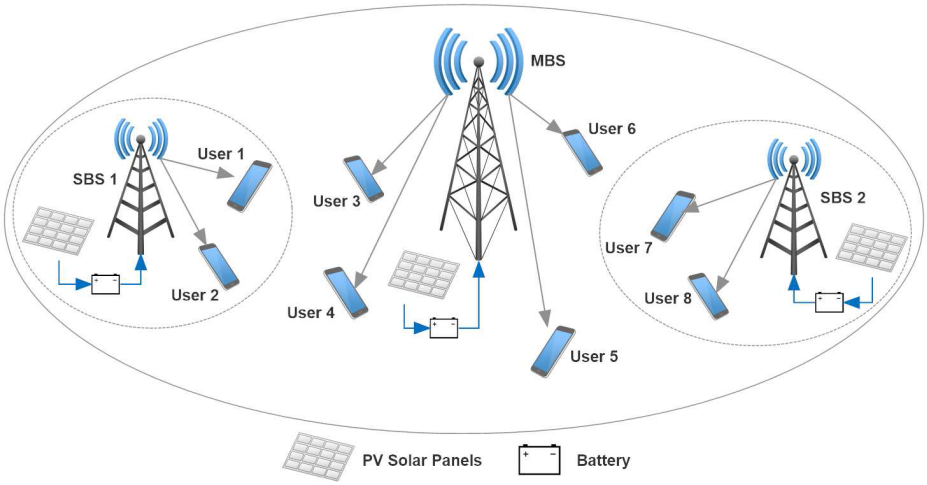

FIGURE 1. A Two-Tier Downlink NOMA HetNet with a MBS and Two SBSs Powered by PV Solar Panels.

For convenience, let $x_{m,i}^k$ be a binary decision variable, defined as

$$x_{m,i}^k = \begin{cases} 1, & \text{if } U_i \in \mathcal{U}_m \text{ is assigned } SC_k \in \mathcal{SC}, \\ 0, & \text{otherwise.} \end{cases} \quad (1)$$

Also, let $E_{m,i}^k$ denote the transmit energy allocated to user U_i within base-station BS_m over subcarrier SC_k. Lastly, let $E^{\max}$ be the total transmit energy per time-slot over each subcarrier $SC_k \in \mathcal{SC}$ (i.e. $\sum_{BS_m \in \mathcal{B}} \sum_{U_i \in \mathcal{U}_m} x_{m,i}^k E_{m,i}^k \leq E^{\max}, \forall SC_k \in \mathcal{SC}$).

B. ENERGY-HARVESTING MODEL

The base-stations are solely powered by renewable energy sources (e.g. via photo-voltaic (PV) solar panels), as shown in Fig. 1. Thus, let τ be a unit-duration time-slot[1], in which downlink NOMA transmission occurs. Additionally, let $\mathcal{E}_m^\tau$ denote the harvested energy from the surrounding environment at $BS_m \in \mathcal{B}$, which is used for downlink transmission. In particular, the harvested energy at each BS_m is modeled as an independent uniform random variable, as $\mathcal{E}_m^\tau \sim \mathbb{U}\left(0, \mathcal{E}_m^{\max}\right)$, with $\mathcal{E}_m^{\max}$ being the maximum value of harvested energy per time-slot [7]. Hence, the total energy consumption over each time-slot τ at each base-station BS_m—for all its associated users and over all subcarriers—must satisfy

$$\sum_{U_i \in \mathcal{U}_m} \sum_{SC_k \in \mathcal{SC}} x_{m,i}^k E_{m,i}^k + E_{C,m} \leq \mathcal{E}_m^\tau, \quad \forall BS_m \in \mathcal{B}, \quad (2)$$

where $E_{C,m}$ is the fixed transceiver energy consumption of the base-station. Additionally, let $B_m^{\max}$ be the finite energy storage device (i.e. battery) of base-station BS_m, $\forall BS_m \in \mathcal{B}$. It should be noted that any leftover energy from a previous time-slot (i.e. $\tau - 1$) is stored in the battery, and used in the following time-slot (for $\tau \geq 2$) along with the harvested energy in that time-slot, as [7]

$$\mathcal{E}_m^\tau = \min\Bigg[\mathcal{E}_m^\tau + \left(\mathcal{E}_m^{\tau-1} - \left(\sum_{U_i \in \mathcal{U}_m} \sum_{SC_k \in \mathcal{SC}} x_{m,i}^k E_{m,i}^k + E_{C,m}\right)\right), B_m^{\max}\Bigg]. \quad (3)$$

If $\mathcal{E}_m^{\tau-1} - \left(\sum_{U_i \in \mathcal{U}_m} \sum_{SC_k \in \mathcal{SC}} x_{m,i}^k E_{m,i}^k + E_{C,m}\right) > 0$, then the excess energy is stored for use in the following time-slot along with the harvested energy. Contrarily, if $\mathcal{E}_m^{\tau-1} - \left(\sum_{U_i \in \mathcal{U}_m} \sum_{SC_k \in \mathcal{SC}} x_{m,i}^k E_{m,i}^k + E_{C,m}\right) = 0$, then there is no excess energy.

Remark 1: For notational convenience, the superscript τ for each time-slot is dropped from this point onwards, while implicitly taking into account battery dynamics during network operation.

C. TRANSMISSION MODEL

Each base-station transmits a superimposed signal of the data symbols of the users associated with it. Thus, the received signal at user $U_i \in \mathcal{U}_m$ of base-station BS_m over subcarrier SC_k is expressed as

$$y_{m,i}^k = \sqrt{E_{m,i}^k} h_{m,i}^k s_{m,i}^k + I_{m,i}^k + J_{m,i}^k + n_{m,i}^k, \quad (4)$$

where $s_{m,i}^k$ is the signal of user $U_i \in \mathcal{U}_m$, such that $\mathbb{E}\left[|s_{m,i}^k|^2\right] = 1$, $\forall U_i \in \mathcal{U}_m$ and $\forall BS_m \in \mathcal{B}$. Moreover, $n_{m,i}^k$ is the received AWGN sample, while $I_{m,i}^k$ is the intra-cell interference, as given by

$$I_{m,i}^k = h_{m,i}^k \sum_{\substack{U_{i'} \in \mathcal{U}_m \\ i' \neq i}} x_{m,i'}^k \sqrt{E_{m,i'}^k} s_{m,i'}^k. \quad (5)$$

[1] In turn, the terms "energy" and "power" can be used interchangeably.

Also, $J^k_{m,i}$ is the inter-cell interference, written as

$$J^k_{m,i} = \sum_{\substack{BS_{m'} \in \mathcal{B} \\ m' \neq m}} h^k_{m',i} \left(\sum_{U_{i'} \in \mathcal{U}_{m'}} x^k_{m',i'} \sqrt{E^k_{m',i'}} s^k_{m',i'} \right). \quad (6)$$

Without loss of generality, let the users in $\mathcal{U}_m$ be ordered in an ascending order according to their *interference channel gains*, as [12]

$$\tilde{h}^k_{m,1} \leq \cdots \leq \tilde{h}^k_{m,i} \leq \cdots \leq \tilde{h}^k_{m,|\mathcal{U}_m|}, \quad (7)$$

where $\tilde{h}^k_{m,i}$ is defined as

$$\tilde{h}^k_{m,i} \triangleq \frac{|h^k_{m,i}|^2}{\mathcal{J}^k_{m,i} + N_0}, \quad (8)$$

and $\mathcal{J}^k_{m,i}$ is inter-cell interference power, as given by

$$\mathcal{J}^k_{m,i} = \sum_{\substack{BS_{m'} \in \mathcal{B} \\ m' \neq m}} |h^k_{m',i}|^2 \left(\sum_{U_{i'} \in \mathcal{U}_{m'}} x^k_{m',i'} E^k_{m',i'} \right). \quad (9)$$

Based on the principle of NOMA [3], [4], the set of users in $\mathcal{U}_m$ are ordered as $E^k_{m,1} \geq \cdots \geq E^k_{m,i} \geq \cdots \geq E^k_{m,|\mathcal{U}_m|}$. Assuming perfect SIC, the received signal-to-interference-plus-noise ratio (SINR) of user $U_i \in \mathcal{U}_m$ over SC_k is determined as

$$\gamma^k_{m,i} = \frac{x^k_{m,i} E^k_{m,i} |h^k_{m,i}|^2}{\mathcal{I}^k_{m,i} + \mathcal{J}^k_{m,i} + N_0}, \quad (10)$$

where $\mathcal{I}^k_{m,i}$ is the intra-cell interference power after SIC, as given by

$$\mathcal{I}^k_{m,i} = |h^k_{m,i}|^2 \left(\sum_{\substack{U_{i'} \in \mathcal{U}_m \\ i' > i}} x^k_{m,i'} E^k_{m,i'} \right). \quad (11)$$

Thus, the achievable rate of user $U_i \in \mathcal{U}_m$ over subcarrier $SC_k \in \mathcal{SC}$ is expressed as

$$R^k_{m,i} \left(\mathbf{E}^k, \mathbf{x}^k \right) = \log_2 \left(1 + \gamma^k_{m,i} \left(\mathbf{E}^k, \mathbf{x}^k \right) \right), \quad (12)$$

where $\mathbf{x}^k \triangleq \left[x^k_{m,i} \right]$ is the network subcarrier assignment matrix over subcarrier SC_k. Also, $\mathbf{E}^k \triangleq \left[E^k_{m,i} \right]$ is the network transmit energy matrix over subcarrier SC_k. Hence, the total achievable rate of user $U_i \in \mathcal{U}_m$ is obtained as

$$R_{m,i} \left(\mathbf{E}, \mathbf{x} \right) = \sum_{SC_k \in \mathcal{SC}} R^k_{m,i} \left(\mathbf{E}^k, \mathbf{x}^k \right), \quad (13)$$

where $\mathbf{x}$ is the network subcarrier assignment matrix; while $\mathbf{E}$ is the network transmit energy matrix. To guarantee quality-of-service (QoS), all network users in each tier must satisfy minimum rate requirements, as

$$R_{m,i} \left(\mathbf{E}, \mathbf{x} \right) \geq \mathbb{R}_{\min}, \quad (14)$$

where

$$\mathbb{R}_{\min} = \begin{cases} \mathbb{R}^M_{\min}, & \forall U_i \in \mathcal{U}_0, \\ \mathbb{R}^S_{\min}, & \forall U_i \in \mathcal{U}_m, \forall m \geq 1, \end{cases} \quad (15)$$

with $\mathbb{R}^M_{\min}$ $\left(\mathbb{R}^S_{\min} \right)$ being the minimum rate requirement per MBS (SBS) user. In turn, the network sum-rate is determined as

$$\begin{aligned} & R_T \left(\mathbf{E}, \mathbf{x} \right) \\ &= \sum_{BS_m \in \mathcal{B}} \left(\sum_{U_i \in \mathcal{U}_m} R_{m,i} \left(\mathbf{E}, \mathbf{x} \right) \right) \\ &= \sum_{BS_m \in \mathcal{B}} \left(\sum_{U_i \in \mathcal{U}_m} \sum_{SC_k \in \mathcal{SC}} \log_2 \left(1 + \frac{x^k_{m,i} E^k_{m,i} |h^k_{m,i}|^2}{\mathcal{I}^k_{m,i} + \mathcal{J}^k_{m,i} + N_0} \right) \right). \end{aligned} \quad (16)$$

On the other hand, the network total energy consumption is given by

$$E_T \left(\mathbf{E}, \mathbf{x} \right) = \sum_{BS_m \in \mathcal{B}} \left(\sum_{U_i \in \mathcal{U}_m} \sum_{SC_k \in \mathcal{SC}} x^k_{m,i} E^k_{m,i} + E_{C,m} \right). \quad (17)$$

Remark 2: In this work, a frequency reuse factor of one is assumed, where all base-stations can transmit over all the subcarriers, and all users can utilize any of the K subcarriers[2].

Remark 3: Each MBS user $U_i \in \mathcal{U}_0$ can be paired to at most ζ^M_i subcarriers (i.e. $\sum_{SC_k \in \mathcal{SC}} x^k_{0,i} \leq \zeta^M_i$). Similarly, each SBS user $U_i \in \mathcal{U}_m$ can be assigned to at most ζ^S_i subcarriers (i.e. $\sum_{SC_k \in \mathcal{SC}} x^k_{m,i} \leq \zeta^S_i, \forall U_i \in \mathcal{U}_m, \forall m \geq 1$).

Remark 4: To reduce SIC complexity and interference, the number of users that can be multiplexed over a subcarrier SC_k in the MBS-tier is constrained to ξ^M_k, while those in the SBS-tier to ξ^S_k. In other words, $\sum_{U_i \in \mathcal{U}_0} x^k_{0,i} \leq \xi^M_k$, and $\sum_{\substack{BS_m \in \mathcal{B} \\ m \geq 1}} \sum_{U_i \in \mathcal{U}_0} x^k_{m,i} \leq \xi^S_k, \forall SC_k \in \mathcal{SC}$.

Remark 5: The SIC receiver complexity per subcarrier in the MBS-tier is $\mathcal{O}\left(\left(\xi^M_k \right)^3 \right)$, while that in the SBS-tier is $\mathcal{O}\left(\left(\xi^S_k \right)^3 \right), \forall SC_k \in \mathcal{SC}$ [4].

In this work, the global energy-efficiency (GEE) is considered, which is defined as the ratio of the network sum-rate to the total energy consumption, as given by (in bits/J/Hz) [17]

$$\textbf{\textit{GEE}} \left(\mathbf{E}, \mathbf{x} \right) \triangleq \frac{R_T \left(\mathbf{E}, \mathbf{x} \right)}{E_T \left(\mathbf{E}, \mathbf{x} \right)}. \quad (18)$$

Remark 6: $\textbf{\textit{GEE}} \left(\mathbf{E}, \mathbf{x} \right)$ is a non-linear and non-convex fractional function.

III. JOINT SUBCARRIER ASSIGNMENT AND GLOBAL ENERGY-EFFICIENT POWER ALLOCATION

The joint subcarrier assignment and global energy-efficient power allocation (J-SA-GEE-PA) problem is formulated as

[2]In turn, users in other cells may be multiplexed over the same subcarrier to maximize spectrum utilization.

J-SA-GEE-PA:

$$\max \quad \textbf{\textit{GEE}}\ (\mathbf{E}, \mathbf{x})$$

$$\text{s.t.} \quad \sum_{BS_m \in \mathcal{B}} \sum_{U_i \in \mathcal{U}_m} x^k_{m,i} E^k_{m,i} \leq E^{\max}, \quad \forall SC_k \in \mathcal{SC}, \tag{19a}$$

$$\sum_{SC_k \in \mathcal{SC}} x^k_{0,i} \leq \zeta^M_i, \quad \forall U_i \in \mathcal{U}_0, \tag{19b}$$

$$\sum_{SC_k \in \mathcal{SC}} x^k_{m,i} \leq \zeta^S_i, \quad \forall U_i \in \mathcal{U}_m,\ \forall m \geq 1, \tag{19c}$$

$$\sum_{U_i \in \mathcal{U}_0} x^k_{0,i} \leq \xi^M_k, \quad \forall SC_k \in \mathcal{SC}, \tag{19d}$$

$$\sum_{BS_m \in \mathcal{B}} \sum_{U_i \in \mathcal{U}_m} x^k_{m,i} \leq \xi^S_k, \quad \forall SC_k \in \mathcal{SC}, \tag{19e}$$

$$R_{0,i}\ (\mathbf{E}, \mathbf{x}) \geq \mathbb{R}^M_{\min}, \quad \forall U_i \in \mathcal{U}_0, \tag{19f}$$

$$R_{m,i}\ (\mathbf{E}, \mathbf{x}) \geq \mathbb{R}^S_{\min}, \quad \forall U_i \in \mathcal{U}_m,\ \forall m \geq 1, \tag{19g}$$

$$E^k_{m,1} \geq \cdots \geq E^k_{m,i} \geq \cdots \geq E^k_{m,|\mathcal{U}_m|}, \quad \forall SC_k \in \mathcal{SC}, \quad \forall BS_m \in \mathcal{B}, \tag{19h}$$

$$\sum_{U_i \in \mathcal{U}_m} \sum_{SC_k \in \mathcal{SC}} x^k_{m,i} E^k_{m,i} + E_{C,m} \leq \mathcal{E}_m, \quad \forall BS_m \in \mathcal{B}, \tag{19i}$$

$$0 \leq E^k_{m,i} \leq x^k_{m,i} E^{\max}, \quad \forall SC_k \in \mathcal{SC}, \quad \forall U_i \in \mathcal{U}_m, \quad \forall BS_m \in \mathcal{B}, \tag{19j}$$

$$x^k_{m,i} \in \{0, 1\}, \quad \forall SC_k \in \mathcal{SC}, \quad \forall U_i \in \mathcal{U}_m,\ \forall BS_m \in \mathcal{B}. \tag{19k}$$

Constraint (19a) ensures that the sum of transmit energy over each subcarrier $SC_k \in \mathcal{SC}$ does not exceed $E^{\max}$. Constraints (19b) and (19c) ensure that no user in the MBS-tier (SBS-tier) is assigned more than ζ^M_i (ζ^S_i) subcarriers. Constraints (19d) and (19e) ensure that the number of MBS (SBS) users multiplexed over any subcarrier $SC_k \in \mathcal{SC}$ does not exceed ξ^M_k (ξ^S_k). Constraints (19f) and (19g) enforce the minimum requirement per MBS and SBS user, respectively, whereas Constraint (19h) enforces the SIC decoding order over each subcarrier within each base-station. Constraint (19i) ensures that the total energy consumption of each base-station does not exceed the available harvested energy. Constraint (19j) ensures that if a user is assigned to a subcarrier (i.e. $x^k_{m,i} = 1$), then its transmit energy $E^k_{m,i}$ does not exceed $E^{\max}$; otherwise, $E^k_{m,i} = 0$. The last constraint defines the values the binary decision variables take.

Remark 7: Problem **J-SA-GEE-PA** is a mixed-integer non-linear fractional programming problem, which can be classified as a mixed-integer non-linear programming (MINLP) problem. More importantly, it is non-convex and NP-hard [14].

Remark 8: Problem **J-SA-GEE-PA** requires $N \cdot K$ binary decision variables and the same for continuous decision variables. Also, it involves a total of $2N + 3K + 2\ N \cdot K + (M + 1) + K \cdot \sum_{BS_m \in \mathcal{B}} (|\mathcal{U}_m| - 1)$ constraints.

Based on **Remarks 7** and **8**, solving problem **J-SA-GEE-PA** is computationally-prohibitive, and there is no known computationally-efficient approach to optimally solve it. Alternatively, problem **J-SA-GEE-PA** can be solved by decoupling it into a two sub-problems: (1) subcarrier assignment via many-to-many matching, and (2) GEE-maximizing power allocation, which are solved over two stages. Specifically, in Stage 1, the aim is to assign the subcarriers to the MBS-tier users, and then optimize their GEE-maximizing power allocation. In Stage 2, the SBS-tier users are assigned to subcarriers, which is followed by GEE-maximizing power allocation for the whole network.

IV. SUBCARRIER ASSIGNMENT VIA MANY-TO-MANY STABLE MATCHING

In this section, the subcarrier assignment sub-problem is modeled as a two-sided many-to-many matching problem [18], [19]. Particularly, the goal is to determine the preference lists of the users within each base-station over the set of acceptable subcarriers, and also the preference lists of the subcarriers over the set of acceptable users within each base-station. After that, a stable matching algorithm—based on the Gale-Shapley deferred acceptance (DA) mechanism [15], [20]—is executed to solve the subcarrier assignment problem in each tier. Specifically, the DA algorithm will used to assign subcarriers to the users in the MBS-tier, and then the users in the SBS-tier. To this end, a few definitions must first be stated [21], [22].

A. DEFINITIONS

Definition 1 (Preference Relations): Each network user $U_i \in \mathcal{U}$ has a strict and transitive preference relation $\succ_U$ over the set $\mathcal{SC} \cup \{\emptyset\}$, while each subcarrier $SC_k \in \mathcal{SC}$ has a strict and transitive preference relation $\succ_{SC_k}$ over $\mathcal{U} \cup \{\emptyset\}$, where $\emptyset$ denotes the possibility of a user (or subcarrier) remaining unassigned[3].

Definition 2 (Acceptability): A subset of the MBS users $\overline{\mathcal{U}}_0 \subseteq \mathcal{U}_0$ is said to be acceptable to subcarrier $SC_k \in \mathcal{SC}$ if and only if (iff) $\sum_{U_i \in \overline{\mathcal{U}}_0} E^k_{0,i} \leq E^{\max}$. Similarly, and given the assigned MBS users, a subset of SBS users $\overline{\mathcal{U}}_m \subseteq \mathcal{U}_m$ within each SBS ($\forall m \geq 1$) is deemed acceptable to subcarrier SC_k iff $\sum_{U_i \in \overline{\mathcal{U}}_0} E^k_{0,i} + \sum_{\substack{BS_m \in \mathcal{B} \\ m \geq 1}} \sum_{U_i \in \overline{\mathcal{U}}_m} E^k_{m,i} \leq E^{\max}$. Also, a subset of subcarriers is said to be acceptable to a MBS user $U_i \in \mathcal{U}_0$ iff $R_{0,i}\ (\mathbf{E}, \mathbf{x}) \geq \mathbb{R}^M_{\min}$ over that subset. In a similar fashion, a subset of subcarriers is deemed acceptable to a SBS user $U_i \in \mathcal{U}_m$ (for $m \geq 1$) iff $R_{m,i}\ (\mathbf{E}, \mathbf{x}) \geq \mathbb{R}^S_{\min}$ over that subset.

Intuitively, the higher the achievable rate of each user over a subset of subcarriers is, the more preferred that subset is. This is in alignment with the selfish nature of the users, aiming at maximizing their individual rates. On the other hand, the lower the sum of transmit energy of a subset of users over a subcarrier is, the more preferred that subset is to

[3]Strictness is implied by the fact that the probability of two channel coefficients being equal is zero, as they are continuous random variables. Thus, the resulting rate values (and total interference power) of each user and subcarrier are distinct. As for the transitivity, it is a direct result of the strictness of the preferences.

that subcarrier. This coincides with each base-station's goal to minimize the energy consumption, and preserve its harvested energy.

Definition 3 (Preference Lists): Let $\mathcal{P}_{U_i}$ be the preference list of user $U_i \in \mathcal{U}_m$ ($\forall BS_m \in \mathcal{B}$), which contains the subsets of acceptance subcarriers in descending order. Similarly, let $\mathcal{P}_{SC_k}$ be the preference list of subcarrier $SC_k \in \mathcal{SC}$, where the subsets of acceptable users are ordered in a descending manner.

Definition 4 (Matching-MBS): A matching in the MBS-tier is a mapping $\mathcal{M}^M \in \mathcal{U}_0 \times \mathcal{SC}$, such that[4]:

(1) $U_i \in \mathcal{M}^M(SC_k)$ iff $SC_k \in \mathcal{M}^M(U_i)$ (i.e. U_i and SC_k are assigned to each other under $\mathcal{M}^M$), $\forall SC_k \in \mathcal{SC}$, $\forall U_i \in \mathcal{U}_0$.
(2) $\left|\mathcal{M}^M(U_i)\right| \leq \zeta_i^M, \forall U_i \in \mathcal{U}_0$.
(3) $\left|\mathcal{M}^M(SC_k)\right| \leq \xi_k^M, \forall SC_k \in \mathcal{SC}$.

Definition 5 (Matching-SBS): A matching in the SBS-tier is a mapping $\mathcal{M}^S \in \overline{\mathcal{U}} \times \mathcal{SC}$, such that[5]:

(1) $U_i \in \mathcal{M}^S(SC_k)$ iff $SC_k \in \mathcal{M}^S(U_i)$, $\forall SC_k \in \mathcal{SC}$, $\forall U_i \in \mathcal{U}_m, \forall m \geq 1$.
(2) $\left|\mathcal{M}^S(U_i)\right| \leq \zeta_i^S, \forall U_i \in \mathcal{U}_m, \forall m \geq 1$.
(3) $\left|\mathcal{M}^S(SC_k)\right| \leq \xi_k^S, \forall SC_k \in \mathcal{SC}$.

Definition 6 (Individual Blocking): A matching $\mathcal{M}$ is said to be blocked by a subcarrier SC_k if there exists some user $U_i \in \mathcal{M}(SC_k)$, such that $\emptyset \succ_{SC_k} U_i$. Similarly, a matching is blocked by a user U_i if there exists some subcarrier $SC_k \in \mathcal{M}(U_i)$, such that $\emptyset \succ_{U_i} SC_k$. In turn, a matching is individually rational if it is not blocked by any user or subcarrier [22].

Definition 7 (Pair Blocking): A matching $\mathcal{M}$ is said to be blocked by a pair (U_i, SC_k) if they are not assigned under $\mathcal{M}$, and:

(1) subcarrier $SC_k \in \mathcal{SC}$ finds U_i acceptable iff U_i finds SC_k acceptable,
(2) $|\mathcal{M}(U_i)| < \zeta_i$, or $SC_k \succ_{U_i} SC_l$, for some $SC_l \in \mathcal{M}(U_i)$, or
(3) $|\mathcal{M}(SC_k)| < \xi_k$, or $U_i \succ_{SC_k} U_j$, for some $U_j \in \mathcal{M}(SC_k)$,

where it should be noted that $\zeta_i = \zeta_i^M$ for a MBS user, while $\zeta_i = \zeta_i^S$ for a SBS user. Similarly, $\xi_k = \xi_k^M$ for users in the MBS-tier, while $\xi_k = \xi_k^S$ for users in the SBS-tier.

Definition 8 (Stability): A matching $\mathcal{M}$ is said to be stable if is not blocked by any individual or any (user, subcarrier) pair [22], and is denoted $\overline{\mathcal{M}}$.

Definition 9 (Max-Min Criterion)[6]*:* Let $\widehat{\mathcal{SC}}$ and $\widetilde{\mathcal{SC}}$ be two subsets of acceptable subcarriers, with $|\widehat{\mathcal{SC}}| \leq \zeta_i$ and $|\widetilde{\mathcal{SC}}| \leq \zeta_i$. Then, a user U_i's preference list is said to satisfy the *max-min criterion* if[7] $|\widehat{\mathcal{SC}}| \geq |\widetilde{\mathcal{SC}}|$ and $\min(\widehat{\mathcal{SC}}) \succ_{U_i} \min(\widetilde{\mathcal{SC}})$ [23]. Similarly, the preference list of a subcarrier is said to satisfy the max-min criterion if the above conditions are analogously satisfied.

Definition 10 (Extended Max-Min Criterion): A user U_i's preference list is said to satisfy the *extended max-min criterion* if—for $\widehat{\mathcal{SC}}$ and $\widetilde{\mathcal{SC}}$ with $|\widehat{\mathcal{SC}}| \leq \zeta_i$ and $|\widetilde{\mathcal{SC}}| \leq \zeta_i$—one of the following conditions holds [21]:

(1) $\widetilde{\mathcal{SC}}$ is a proper subset of $\widehat{\mathcal{SC}}$ (i.e. $\widetilde{\mathcal{SC}} \subset \widehat{\mathcal{SC}}$), or
(2) $|\widehat{\mathcal{SC}}| > |\widetilde{\mathcal{SC}}|$ and $\min(\widehat{\mathcal{SC}}) \succ_{U_i} \min(\widetilde{\mathcal{SC}})$.

In a similar fashion, the preference list of a subcarrier is said to satisfy the extended max-min criterion if the above conditions are met.

In the max-min criterion, the subset $\widehat{\mathcal{SC}}$ may not be strictly preferable to its subset $\widetilde{\mathcal{SC}}$; however, this is not the case for the extended max-min criterion. That is, the extended max-min criterion ensures that users always want to be assigned to as many subcarriers as possible within their quotas. Similarly, the subcarriers wish to be assigned to as many users as possible within their quotas. This is intuitive from the perspective of efficiently and optimally utilizing network resources.

Remark 9: In this work, the extended max-min criterion is considered, and the max-min criterion has only been stated for completeness.

Definition 11 (Substitutability): Let $\mathcal{C}\left(\mathcal{SC}, \mathcal{P}_{U_i}\right)$ denote the most preferred subset of $\mathcal{SC}$ for user U_i according to its preference list $\mathcal{P}_{U_i}$. Similarly, let $\mathcal{C}\left(\mathcal{U}, \mathcal{P}_{SC_k}\right)$ be the most preferred subset of $\mathcal{U}$ by subcarrier $SC_k \in \mathcal{SC}$, as per its preference list $\mathcal{P}_{SC_k}$. Then, a user's preference list $\mathcal{P}_{U_i}$ satisfies *substitutability* for any set $\mathcal{SC}$ containing subcarriers SC_k and SC_l (for $k \neq l$), if $SC_k \in \mathcal{C}\left(\mathcal{SC}, \mathcal{P}_{U_i}\right)$, then $SC_k \in \mathcal{C}\left(\mathcal{SC} \setminus \{SC_l\}, \mathcal{P}_{U_i}\right)$ [24]. In a similar manner, a subcarrier's preference list $\mathcal{P}_{SC_k}$ is said to satisfy *substitutability* for any set $\mathcal{U}$ containing users U_i and U_j (for $i \neq j$), if $U_i \in \mathcal{C}\left(\mathcal{U}, \mathcal{P}_{SC_k}\right)$, then $U_i \in \mathcal{C}\left(\mathcal{U} \setminus \{U_j\}, \mathcal{P}_{SC_k}\right)$.

Simply put, substitutability states that if assigning a subcarrier $SC_k \in \mathcal{SC}$ (a user $U \in \mathcal{U}$) to a user (subcarrier) is optimal when a certain set of subcarriers (users) is available, then assigning SC_k (U) to the same user (subcarrier) must also be optimal when a subset of subcarriers (users) is available [21].

Remark 10: The extended max-min criterion implies substitutability [21], [23].

B. ALGORITHM DESCRIPTION

In this subsection, the DA algorithm is devised. Particularly, each user $U_i \in \mathcal{U}_m$ proposes to its most preferred ζ_i acceptable subcarriers. Then, each subcarrier $SC_k \in \mathcal{SC}$ places the ξ_k most preferred users on its waiting list, and rejects the rest. Any rejected user U_i in the previous step proposes again to its most preferred ζ_i acceptable subcarriers, provided that none of the proposed-to subcarriers have previously rejected that user (i.e. no user proposes twice to the same subcarrier). After that, each subcarrier SC_k selects the best ξ_k users from

[4]Generally speaking, $\mathcal{M}(U_i)$ denotes the subset of subcarriers assigned to user $U_i \in \mathcal{U}_m$, while $\mathcal{M}(SC_k)$ denotes the subset of users assigned to subcarrier SC_k.

[5]Note that $\overline{\mathcal{U}} \triangleq \mathcal{U} \backslash \mathcal{U}_0$ (or equivalently $\overline{\mathcal{U}} = \bigcup_{m=1}^{M} \mathcal{U}_m$), which represents the subset of all SBS users.

[6]The "max" term implies that all users want to be assigned to as many subcarriers as possible, while the "min" term indicates that the users focus on the worst subcarrier when ranking the subcarriers, and vice versa.

[7]In general, $\min(\mathcal{SC})$ denotes the least preferred subcarrier in the set $\mathcal{SC}$. Similarly $\min(\mathcal{U})$ resembles the least preferred user in the set $\mathcal{U}$.

among the newly proposing users and those already on its waiting list, updates its waiting list, and rejects the rest. This process repeats until convergence, yielding the stable matching solution $\overline{\mathcal{M}}$, as given in Algorithm 1.

Algorithm 1 Deferred Acceptance (DA)

Input: Preference lists $\mathcal{P}_{U_i}$ and $\mathcal{P}_{SC_k}$, $\forall SC_k \in \mathcal{SC}$, $\forall U_i \in \mathcal{U}_m$.

1: Each user $U_i \in \mathcal{U}_m$ proposes to its most preferred ζ_i acceptable subcarriers in $\mathcal{SC}$;
2: Each subcarrier $SC_k \in \mathcal{SC}$ places on its waiting list the ξ_k most preferred users, and rejects the rest;
3: WHILE (there exists a previously rejected user $U_i \in \mathcal{U}_m$ with a non-empty preference list that contains at least one subcarrier that has not rejected it before)
4: Any user $U_i \in \mathcal{U}_m$ that was previously rejected by any subcarrier proposes to its most preferred ζ_i acceptable subcarriers, which have not previously rejected it;
5: Each subcarrier $SC_k \in \mathcal{SC}$ selects the best ξ_k users from among the newly proposing users and those on its waiting list, places them on its waiting list, and rejects the rest;
6: END WHILE

Output: Stable matching solution $\overline{\mathcal{M}}$.

Remark 11: The proposed **DA** algorithm is applicable to the MBS- and SBS-tiers. Specifically, for the MBS-tier, the preference lists of all users associated with the MBS (i.e. $U_i \in \mathcal{U}_0$) are utilized to obtain the MBS stable matching solution, denoted $\overline{\mathcal{M}}^M$, while satisfying ζ_i^M, $\forall U_i \in \mathcal{U}_0$, and ξ_k^M, $\forall SC_k \in \mathcal{SC}$. As for the SBS-tier, the preference lists of all users within all SBSs (i.e. excluding the MBS users, and hence $\overline{\mathcal{U}} = \mathcal{U} \setminus \mathcal{U}_0$) are utilized to obtain the SBS stable matching solution, denoted $\overline{\mathcal{M}}^S$, while satisfying ζ_i^S, $\forall U_i \in \mathcal{U}_m$ ($\forall m \geq 1$), and ξ_k^S, $\forall SC_k \in \mathcal{SC}$.

C. PROPERTIES

1) EXISTENCE:

Lemma 1: Every instance of the **DA** algorithm yields at least one stable matching solution.

Proof: Refer to Appendix A. ■

2) CONVERGENCE:

Lemma 2: The **DA** algorithm converges in a finite number of iterations to a stable matching solution $\overline{\mathcal{M}}$.

Proof: Refer to Appendix B. ■

3) COMPLEXITY:

In general, the **DA** algorithm has a worst-case polynomial-time complexity of $\mathcal{O}\left(L^2\right)$, where $L = \max\left(N, K\right)$, with N and K being the number of users and subcarriers, respectively [15], [19], [25]. Specifically, for the MBS-tier, $L = \max\left(|\mathcal{U}_0|, K\right)$, while for the SBS-tier, $L = \max\left(|\overline{\mathcal{U}}|, K\right)$.

4) UNIQUENESS:

Lemma 3: Given that the extended max-min criterion holds, the **DA** algorithm converges to the unique stable matching solution $\overline{\mathcal{M}}$ [21].

Proof: Refer to Appendix C. ■

Remark 12: The **DA** algorithm along with the extended max-min criterion maximize the cardinality of the subcarrier assignment solution.

V. GLOBAL ENERGY-EFFICIENT POWER ALLOCATION

In this section, the global energy-efficient power allocation problem over the two stages is studied.

A. STAGE 1

After executing the proposed **DA** algorithm, the subcarriers are assigned to the MBS-tier users only, which implies that no SBS-tier users are assigned to the subcarriers yet, and thus no inter-cell interference. Let $\bar{\mathbf{x}}^M = \left[\bar{x}_{0,i}^k\right]$ (for $\bar{x}_{0,i}^k \in \{0, 1\}$) be the subcarrier assignment of the MBS users, obtained via **DA** algorithm (i.e. $\bar{\mathbf{x}}^M = \overline{\mathcal{M}}^M$). Hence, the global energy-efficient power allocation in Stage 1 (GEE-PA-Stage-1) for *fixed* MBS users' subcarrier assignment is formulated as[8]

GEE-PA-Stage-1:

$$\max \ \boldsymbol{GEE}\left(\mathbf{E}^M, \bar{\mathbf{x}}^M\right)$$

$$\text{s.t.} \sum_{U_i \in \mathcal{U}_0} \bar{x}_{0,i}^k E_{0,i}^k \leq E^{\max}, \ \forall SC_k \in \mathcal{SC}, \tag{20a}$$

$$R_{0,i}\left(\mathbf{E}^M, \bar{\mathbf{x}}^M\right) \geq \mathbb{R}_{\min}^M, \ \forall U_i \in \mathcal{U}_0, \tag{20b}$$

$$E_{0,1}^k \geq \cdots \geq E_{0,i}^k \geq \cdots \geq E_{0,|\mathcal{U}_0|}^k, \ \forall SC_k \in \mathcal{SC}, \tag{20c}$$

$$\sum_{U_i \in \mathcal{U}_0} \sum_{SC_k \in \mathcal{SC}} \bar{x}_{0,i}^k E_{0,i}^k + E_{C,0} \leq \mathcal{E}_0, \tag{20d}$$

$$0 \leq E_{0,i}^k \leq \bar{x}_{0,i}^k E^{\max}, \ \forall U_i \in \mathcal{U}_0, \ \forall SC_k \in \mathcal{SC}, \tag{20e}$$

where

$$\begin{aligned} &\boldsymbol{GEE}\left(\mathbf{E}^M, \bar{\mathbf{x}}^M\right) \\ &= \frac{\sum_{U_i \in \mathcal{U}_0} \sum_{SC_k \in \mathcal{SC}} \log_2\left(1 + \frac{\bar{x}_{0,i}^k E_{0,i}^k |h_{0,i}^k|^2}{\mathcal{I}_{0,i}^k + N_0}\right)}{\sum_{U_i \in \mathcal{U}_0} \sum_{SC_k \in \mathcal{SC}} \bar{x}_{0,i}^k E_{0,i}^k + E_{C,0}} \\ &= \frac{R_T\left(\mathbf{E}^M, \bar{\mathbf{x}}^M\right)}{E_T\left(\mathbf{E}^M, \bar{\mathbf{x}}^M\right)}, \end{aligned} \tag{21}$$

and $\mathbf{E}^M = \left[E_{0,i}^k\right]$ is the transmit energy matrix of the MBS users over the K subcarriers.

Remark 13: Problem **GEE-PA-Stage-1** involves $|\mathcal{U}_0| \cdot K$ continuous decision variables, and a total of $(1+2K)|\mathcal{U}_0|+1$ constraints.

[8]Note that the constraints corresponding to ζ_i^M and ξ_k^M have been eliminated from problem **GEE-PA-Stage-1**, as they have been incorporated into the **DA** algorithm, and thus in the obtained subcarrier assignment solution $\bar{\mathbf{x}}^M = \overline{\mathcal{M}}^M$.

Remark 14: It can be verified that the numerator of $\boldsymbol{GEE}\left(\mathbf{E}^M, \bar{\mathbf{x}}^M\right)$ is not jointly concave in $\mathbf{E}^M$ (i.e. non-convex). This is because $R_{0,i}\left(\mathbf{E}^M, \bar{\mathbf{x}}^M\right)$ is not necessarily concave in $\mathbf{E}^M$, $\forall U_i \in \mathcal{U}_0$, which is mainly due to the intra-cell interference [17], [26]. In turn, problem **GEE-PA-Stage-1** is not convex.

To efficiently solve problem **GEE-PA-Stage-1**, consider the inequality [27]

$$\log_2(1+\gamma) \geq \alpha \log_2(\gamma) + \beta, \tag{22}$$

where

$$\alpha \triangleq \frac{\bar{\gamma}}{\bar{\gamma}+1}, \tag{23}$$

and

$$\beta \triangleq \log_2(1+\bar{\gamma}) - \alpha \log_2(\bar{\gamma}), \tag{24}$$

with $\gamma, \bar{\gamma} > 0$, and the inequality is tight for $\gamma = \bar{\gamma}$. Now, by using the variable substitution $E^k_{0,i} = 2^{Q^k_{0,i}}$, the rate function $R_{0,i}\left(\mathbf{E}^M, \bar{\mathbf{x}}^M\right)$ can be re-written as [26]

$$R_{0,i}\left(\mathbf{Q}^M, \bar{\mathbf{x}}^M\right) = \sum_{SC_k \in \mathcal{SC}} \log_2\left(1 + \frac{\bar{x}^k_{0,i} 2^{Q^k_{0,i}} |h^k_{0,i}|^2}{|h^k_{0,i}|^2 \left(\sum_{\substack{U_{i'} \in \mathcal{U}_0 \\ i'>i}} \bar{x}^k_{0,i'} 2^{Q^k_{0,i'}}\right) + N_0}\right), \tag{25}$$

where $\mathbf{Q}^M \triangleq \left[Q^k_{0,i}\right]$ is the transformed transmit energy matrix of the MBS-tier. Using the inequality in (22), $R_{0,i}\left(\mathbf{Q}^M, \bar{\mathbf{x}}^M\right)$ in (25) is lower-bounded as given in (26), as shown at the bottom of this page.

Remark 15: The negative *log-sum-exp* term

$$-\log_2\left(|h^k_{0,i}|^2 \left(\sum_{\substack{U_{i'} \in \mathcal{U}_0 \\ i'>i}} \bar{x}^k_{0,i'} 2^{Q^k_{0,i'}}\right) + N_0\right)$$

is concave[9] [26]. Since sum of concave functions is also concave [28], then, the lower-bounded rate function $\bar{R}_{0,i}\left(\mathbf{Q}^M, \bar{\mathbf{x}}^M\right)$ can also be verified to be concave in $\mathbf{Q}^M$, for fixed $\bar{\mathbf{x}}^M$.

Based on the above, the $\boldsymbol{GEE}\left(\mathbf{E}, \bar{\mathbf{x}}\right)$ objective function of problem **GEE-PA-Stage-1** is lower-bounded and re-written as given in (27), as shown at the bottom of this page. A similar transformation applies to the remaining constraints in problem **GEE-PA-Stage-1**. Hence, problem **GEE-PA-Stage-1** can be *reformulated* as

R-GEE-PA-Stage-1:

$$\max \quad \overline{\boldsymbol{GEE}}\left(\mathbf{Q}^M, \bar{\mathbf{x}}^M\right)$$

$$\text{s.t.} \quad \sum_{U_i \in \mathcal{U}_0} \bar{x}^k_{0,i} 2^{Q^k_{0,i}} \leq E^{\max}, \ \forall SC_k \in \mathcal{SC}, \tag{28a}$$

$$\bar{R}_{0,i}\left(\mathbf{Q}^M, \bar{\mathbf{x}}^M\right) \geq \mathbb{R}^M_{\min}, \ \forall U_i \in \mathcal{U}_0, \tag{28b}$$

$$Q^k_{0,1} \geq \cdots \geq Q^k_{0,i} \geq \cdots \geq Q^k_{0,|\mathcal{U}_0|}, \ \forall SC_k \in \mathcal{SC}, \tag{28c}$$

$$\sum_{U_i \in \mathcal{U}_0} \sum_{SC_k \in \mathcal{SC}} \bar{x}^k_{0,i} 2^{Q^k_{0,i}} + E_{C,0} \leq \mathcal{E}_0, \tag{28d}$$

$$0 \leq 2^{Q^k_{0,i}} \leq \bar{x}^k_{0,i} E^{\max}, \ \forall U_i \in \mathcal{U}_0, \ \forall SC_k \in \mathcal{SC}. \tag{28e}$$

Remark 16: All the constraints in Problem **R-GEE-PA-Stage-1** can be verified to be convex and/or linear, which implies that the constraints set is convex. Moreover, the objective function is ratio of the concave $\bar{R}_T\left(\mathbf{Q}^M, \bar{\mathbf{x}}^M\right)$ function to the convex $E_T\left(\mathbf{Q}^M, \bar{\mathbf{x}}^M\right)$ function.

Consequently, problem **R-GEE-PA-Stage-1** can be globally optimally solved via Dinkelbach's algorithm [29]. To this end, define the auxiliary function [30]

$$\bar{F}(\lambda) = \max_{\mathbf{Q}^M} \left\{\bar{R}_T\left(\mathbf{Q}^M, \bar{\mathbf{x}}^M\right) - \lambda \bar{E}_T\left(\mathbf{Q}^M, \bar{\mathbf{x}}^M\right)\right\}, \tag{29}$$

where $\lambda \geq 0$ is the unique maximizer of $\bar{F}(\lambda)$, for fixed values of $\alpha^k_{0,i}$ and $\beta^k_{0,i}$, $\forall SC_k \in \mathcal{SC}$, and $\forall U_i \in \mathcal{U}_0$ [31]. The Dinkelbach's algorithm is given in Algorithm 2.

Lemma 4: **Algorithm 2** monotonically improves the values of $\left\{\lambda^{(l)}\right\}_l$, ultimately converging to the global optimal solution $\hat{\mathbf{Q}}^M$ of problem **R-GEE-PA-Stage-1** [32].

Proof: Refer to Appendix D. ∎

Based on **Algorithm 2**[10], the obtained solution $\hat{\mathbf{Q}}^M$ must be converted into its original form as $\hat{\mathbf{E}}^M = 2^{\hat{\mathbf{Q}}^M}$.

[9]The *sum-exp* term can be verified to be convex [28].

[10]**Algorithm 2** has a polynomial-time complexity, and a linear convergence rate [17].

$$R_{0,i}\left(\mathbf{Q}^M, \bar{\mathbf{x}}^M\right) \geq \bar{R}_{0,i}\left(\mathbf{Q}^M, \bar{\mathbf{x}}^M\right) \triangleq \sum_{SC_k \in \mathcal{SC}} \alpha^k_{0,i} \left(Q^k_{0,i} + \log_2\left(\bar{x}^k_{0,i} |h^k_{0,i}|^2\right) - \log_2\left(|h^k_{0,i}|^2 \left(\sum_{\substack{U_{i'} \in \mathcal{U}_0 \\ i'>i}} \bar{x}^k_{0,i'} 2^{Q^k_{0,i'}}\right) + N_0\right)\right) + \beta^k_{0,i}. \tag{26}$$

$$\boldsymbol{GEE}\left(\mathbf{E}^M, \bar{\mathbf{x}}^M\right) \geq \overline{\boldsymbol{GEE}}\left(\mathbf{Q}^M, \bar{\mathbf{x}}^M\right) = \frac{\sum_{U_i \in \mathcal{U}_0} \bar{R}_{0,i}\left(\mathbf{Q}^M, \bar{\mathbf{x}}^M\right)}{\sum_{U_i \in \mathcal{U}_0} \sum_{SC_k \in \mathcal{SC}} \bar{x}^k_{0,i} 2^{Q^k_{0,i}} + E_{C,0}} \triangleq \frac{\bar{R}_T\left(\mathbf{Q}^M, \bar{\mathbf{x}}^M\right)}{\bar{E}_T\left(\mathbf{Q}^M, \bar{\mathbf{x}}^M\right)}. \tag{27}$$

Algorithm 2 Dinkelbach's Algorithm for Solving Problem **R-GEE-PA-Stage-1**

Set $\epsilon \in (0,1)$, $l=0$, and $\lambda^{(0)}=0$.
1: WHILE $\bar{F}\left(\lambda^{(l)}\right) > \epsilon$
2: $\tilde{\mathbf{Q}}^{(l)} = \arg\max_{\mathbf{Q}} \left\{\bar{R}_T\left(\mathbf{Q}, \bar{\mathbf{x}}^M\right) - \lambda^{(l)}\bar{E}_T\left(\mathbf{Q}, \bar{\mathbf{x}}^M\right)\right\}$;
3: $\bar{F}\left(\lambda^{(l)}\right) = \bar{R}_T\left(\tilde{\mathbf{Q}}^{(l)}, \bar{\mathbf{x}}^M\right) - \lambda^{(l)}\bar{E}_T\left(\tilde{\mathbf{Q}}^{(l)}, \bar{\mathbf{x}}^M\right)$;
4: $\lambda^{(l+1)} = \frac{\bar{R}_T\left(\tilde{\mathbf{Q}}^{(l)}, \bar{\mathbf{x}}^M\right)}{\bar{E}_T\left(\tilde{\mathbf{Q}}^{(l)}, \bar{\mathbf{x}}^M\right)}$;
5: $l = l+1$;
6: END WHILE
Output: $\hat{\mathbf{Q}}^M \triangleq \tilde{\mathbf{Q}}^*$.

Hence, the value of the objective function in (21)–for fixed values of $\alpha_{0,i}^k$ and $\beta_{0,i}^k$—is obtained as

$$\widehat{\boldsymbol{GEE}}\left(\hat{\mathbf{E}}^M, \bar{\mathbf{x}}^M\right) \triangleq \frac{\sum_{U_i\in\mathcal{U}_0} R_{0,i}\left(\hat{\mathbf{E}}^M, \bar{\mathbf{x}}^M\right)}{\sum_{U_i\in\mathcal{U}_0}\sum_{SC_k\in\mathcal{SC}} \bar{x}_{0,i}^k \hat{E}_{0,i}^k + E_{C,0}}. \tag{30}$$

Recall that the objective function value obtained via **Algorithm 2** is a lower-bound, and thus, it must be improved by repeatedly updating $\alpha_{0,i}^k$ and $\beta_{0,i}^k$ as per (23) and (24), $\forall SC_k \in \mathcal{SC}$, and $\forall U_i \in \mathcal{U}_0$. This is achieved via Algorithm 3, ultimately yielding the transmit energy matrix $\bar{\mathbf{E}}^M$.

Algorithm 3 Solution of Problem **GEE-PA-Stage-1**

Set $\epsilon \in (0,1)$, $l=0$, find a feasible $\hat{\mathbf{E}}^{(0)}$, and set $\alpha_{0,i}^{k,(0)} = 1$ and $\beta_{0,i}^{k,(0)} = 0$, $\forall SC_k \in \mathcal{SC}$, and $\forall U_i \in \mathcal{U}_0$.
1: WHILE $\left|\widehat{GEE}\left(\hat{\mathbf{E}}^{(l+1)}, \bar{\mathbf{x}}^M\right) - \widehat{GEE}\left(\hat{\mathbf{E}}^{(l)}, \bar{\mathbf{x}}^M\right)\right| > \epsilon$
2: $l = l+1$;
3: Evaluate $\widehat{GEE}\left(\hat{\mathbf{E}}^{(l)}, \bar{\mathbf{x}}^M\right)$;
4: Update $\alpha_{0,i}^{k,(l)}$ and $\beta_{0,i}^{k,(l)}$, $\forall SC_k \in \mathcal{SC}$, and $\forall U_i \in \mathcal{U}_0$;
5: Obtain $\hat{\mathbf{Q}}^{(l)}$ by solving **R-GEE-PA-Stage-1** via **Algorithm 2**;
6: Set $\hat{\mathbf{E}}^{(l)} = 2^{\hat{\mathbf{Q}}^{(l)}}$;
7: END WHILE
Output: $\bar{\mathbf{E}}^M \triangleq \hat{\mathbf{E}}^*$.

Lemma 5: The sequence of objective function values $\left\{\widehat{\boldsymbol{GEE}}\left(\hat{\mathbf{E}}^{(l)}, \bar{\mathbf{x}}^M\right)\right\}_l$ increases monotonically, and converges to the optimal solution $\bar{\mathbf{E}}^M$ of problem **GEE-PA-Stage-1**—satisfying Karush-Kuhn-Tucker (KKT) conditions—in a finite number of iterations.

Proof: Refer to Appendix E. ∎

B. STAGE 2

Let the subcarrier assignment of the users in the SBS-tier be denoted by $\bar{\mathbf{x}}^S$ (i.e. $\bar{\mathbf{x}}^S = \mathcal{M}^S$), which is obtained by the **DA** algorithm. Here, the aim is to optimize the network transmit energy of all users (in the MBS- and SBS-tiers), while ensuring that the MBS-tier users do not violate their minimum rate requirements due to the subcarriers' re-use by the SBS users. This is because allocating the subcarriers to the SBS users introduces inter-cell interference, and hence the MBS-tier users may potentially violate their minimum rate constraints. In other words, after the SBS users' subcarrier assignment, the GEE-PA may no longer be optimal with respect to the MBS users.

For notational convenience, let $\bar{\mathbf{x}} \triangleq \left(\bar{\mathbf{x}}^M, \bar{\mathbf{x}}^S\right)$—which corresponds to $\overline{\mathcal{M}} = \overline{\mathcal{M}}^M \cup \overline{\mathcal{M}}^S$—be the fixed subcarrier assignment of all network users. Hence, in Stage 2, problem **J-SA-GEE-PA** reduces to

GEE-PA-Stage-2:

$$\max \quad \boldsymbol{GEE}\left(\mathbf{E}, \bar{\mathbf{x}}\right)$$
$$\text{s.t.} \quad \sum_{BS_m\in\mathcal{B}}\sum_{U_i\in\mathcal{U}_m} \bar{x}_{m,i}^k E_{m,i}^k \le E^{\max}, \quad \forall SC_k \in \mathcal{SC}, \tag{31a}$$
$$R_{0,i}\left(\mathbf{E}, \bar{\mathbf{x}}^M\right) \ge \mathbb{R}_{\min}^M, \ \forall U_i \in \mathcal{U}_0, \tag{31b}$$
$$R_{m,i}\left(\mathbf{E}, \bar{\mathbf{x}}^S\right) \ge \mathbb{R}_{\min}^S, \ \forall U_i \in \mathcal{U}_m, \quad \forall m \ge 1, \tag{31c}$$
$$E_{m,1}^k \ge \cdots \ge E_{m,i}^k \ge \cdots \ge E_{m,|\mathcal{U}_m|}^k, \quad \forall SC_k \in \mathcal{SC}, \quad \forall BS_m \in \mathcal{B}, \tag{31d}$$
$$\sum_{U_i\in\mathcal{U}_m}\sum_{SC_k\in\mathcal{SC}} \bar{x}_{m,i}^k E_{m,i}^k + E_{C,m} \le \mathcal{E}_m, \quad \forall BS_m \in \mathcal{B}, \tag{31e}$$
$$0 \le E_{m,i}^k \le \bar{x}_{m,i}^k E^{\max}, \quad \forall SC_k \in \mathcal{SC}, \forall U_i \in \mathcal{U}_m, \forall BS_m \in \mathcal{B}. \tag{31f}$$

Additionally,

$$\boldsymbol{GEE}\left(\mathbf{E}, \bar{\mathbf{x}}\right) = \frac{\sum_{BS_m\in\mathcal{B}}\left(\sum_{U_i\in\mathcal{U}_m}\sum_{SC_k\in\mathcal{SC}} \log_2\left(1 + \frac{\bar{x}_{m,i}^k E_{m,i}^k |h_{m,i}^k|^2}{\mathcal{I}_{m,i}^k + \mathcal{J}_{m,i}^k + N_0}\right)\right)}{\sum_{BS_m\in\mathcal{B}}\left(\sum_{U_i\in\mathcal{U}_m}\sum_{SC_k\in\mathcal{SC}} \bar{x}_{m,i}^k E_{m,i}^k + E_{C,m}\right)} = \frac{R_T\left(\mathbf{E}, \bar{\mathbf{x}}\right)}{E_T\left(\mathbf{E}, \bar{\mathbf{x}}\right)}. \tag{32}$$

Remark 17: Problem **GEE-PA-Stage-2** involves a total $N \cdot K$ continuous decision variables, and $N + K + N \cdot K + (M+1) + K \cdot \sum_{BS_m\in\mathcal{B}}(|\mathcal{U}_m| - 1)$ constraints.

As before, it can be verified that problem **GEE-PA-Stage-2** is not convex, where the non-convexity results from the non-convex rate functions (due to the intra- and inter-cell interference terms). Thus, the objective function is also non-convex. By utilizing the inequality in (22), and the variable substitution $E_{m,i}^k = 2^{Q_{m,i}^k}$, problem **GEE-PA-Stage-2** can be reformulated as

R-GEE-PA-Stage-2:

$$\max \quad \overline{\overline{\boldsymbol{GEE}}}\left(\mathbf{Q}, \bar{\mathbf{x}}\right)$$
$$\text{s.t.} \quad \sum_{BS_m\in\mathcal{B}}\sum_{U_i\in\mathcal{U}_m} \bar{x}_{m,i}^k 2^{Q_{m,i}^k} \le E^{\max}, \ \forall SC_k \in \mathcal{SC}, \tag{33a}$$
$$\bar{\bar{R}}_{m,i}\left(\mathbf{Q}, \bar{\mathbf{x}}\right) \ge \mathbb{R}_{\min}^M, \ \forall U_i \in \mathcal{U}_0, \tag{33b}$$
$$\bar{\bar{R}}_{m,i}\left(\mathbf{Q}, \bar{\mathbf{x}}\right) \ge \mathbb{R}_{\min}^S, \ \forall U_i \in \mathcal{U}_m, \forall m \ge 1, \tag{33c}$$

$$Q^k_{m,1} \geq \cdots \geq Q^k_{m,i} \geq \cdots \geq Q^k_{m,|\mathcal{U}_m|}, \quad \forall SC_k \in \mathcal{SC}, \forall BS_m \in \mathcal{B}, \tag{33d}$$

$$\sum_{U_i \in \mathcal{U}_m} \sum_{SC_k \in \mathcal{SC}} \bar{x}^k_{m,i} 2^{Q^k_{m,i}} + E_{C,m} \leq \mathcal{E}_m, \ \forall BS_m \in \mathcal{B}, \tag{33e}$$

$$0 \leq 2^{Q^k_{m,i}} \leq \bar{x}^k_{m,i} E^{\max}, \quad \forall SC_k \in \mathcal{SC}, \forall U_i \in \mathcal{U}_m, \forall BS_m \in \mathcal{B}, \tag{33f}$$

where

$$\overline{\overline{\boldsymbol{GEE}}}\left(\mathbf{Q}, \bar{\mathbf{x}}\right) = \frac{\sum_{BS_m \in \mathcal{B}} \left(\sum_{U_i \in \mathcal{U}_m} \bar{\bar{R}}_{m,i}\left(\mathbf{Q}, \bar{\mathbf{x}}\right) \right)}{\sum_{BS_m \in \mathcal{B}} \left(\sum_{U_i \in \mathcal{U}_m} \sum_{SC_k \in \mathcal{SC}} \bar{x}^k_{m,i} 2^{Q^k_{m,i}} + E_{C,m} \right)} \triangleq \frac{\bar{\bar{R}}_T\left(\mathbf{Q}, \bar{\mathbf{x}}\right)}{\bar{\bar{E}}_T\left(\mathbf{Q}, \bar{\mathbf{x}}\right)} \tag{34}$$

is the lower-bounded objective function, and $\mathbf{Q} = \left[Q^k_{m,i}\right]$ is the network transformed transmit energy matrix. Moreover, $\bar{\bar{R}}_{m,i}\left(\mathbf{Q}, \bar{\mathbf{x}}\right)$ is the lower-bounded rate function, as given by (35), as shown at the bottom of this page, which can be verified to be concave, as per **Remark 15**. In turn, the objective function $\overline{\overline{\boldsymbol{GEE}}}\left(\mathbf{Q}, \bar{\mathbf{x}}\right)$ is a ratio of a concave function to a convex function, and the constraints set can also be verified to be convex. Hence, problem **R-GEE-PA-Stage-2** can also be globally optimally solved via **Algorithm 2** to obtain $\hat{\mathbf{E}} = 2^{\hat{\mathbf{Q}}}$ by using the auxiliary function

$$\bar{\bar{F}}\left(\lambda\right) = \max_{\mathbf{Q}} \left\{ \bar{\bar{R}}_T\left(\mathbf{Q}, \bar{\mathbf{x}}\right) - \lambda \bar{\bar{E}}_T\left(\mathbf{Q}, \bar{\mathbf{x}}\right) \right\}, \tag{36}$$

subject to fixed values of $\alpha^k_{m,i}$ and $\beta^k_{m,i}$, $\forall SC_k \in \mathcal{SC}$, $\forall U_i \in \mathcal{U}_m$, and $\forall BS_m \in \mathcal{B}$. After that, the optimized lower-bounded objective function (denoted $\widehat{\overline{\overline{\boldsymbol{GEE}}}}\left(\hat{\mathbf{E}}, \bar{\mathbf{x}}\right)$) can be iteratively improved by updating the values of $\alpha^k_{m,i}$ and $\beta^k_{m,i}$ via **Algorithm 3**, until convergence to the network transmit energy matrix $\bar{\mathbf{E}}$ of problem **GEE-PA-Stage-2**.

Since the solution of problem **GEE-PA-Stage-2** is based on similar analytical techniques to problem **GEE-PA-Stage-1**, then it suffices to state the following propositions without proof to avoid unnecessary repetition.

Proposition 1: **Algorithm 2** monotonically improves $\left\{\lambda^{(l)}\right\}_l$, and thus converges to the global optimal solution $\hat{\mathbf{Q}}$ of problem **R-GEE-PA-Stage-2**.

Proposition 2: The sequence of objective function values $\left\{\widehat{\overline{\overline{\boldsymbol{GEE}}}}\left(\hat{\mathbf{E}}^{(l)}, \bar{\mathbf{x}}\right)\right\}_l$ increases monotonically, ultimately converging in a finite number of iterations to the optimal solution $\bar{\mathbf{E}}$ of problem **GEE-PA-Stage-2**, satisfying the KKT conditions.

VI. TWO-SIDED EXCHANGE-STABILITY VIA SWAP MATCHING

Considering the aforementioned matching-theoretic subcarrier assignment and GEE-maximizing power allocation algorithms, our resource allocation problem is one with externalities (also known as *peer effects*) [16]. Specifically, the preference lists of the users and subcarriers in the MBS-tier are initially constructed using a feasible transmit energy matrix, without accounting for intra-cell interference over each subcarrier. This is due to the fact that no subcarrier assignment initially exists in the MBS-tier, and hence intra-cell interference is not accounted for in the construction of the preference lists of the MBS users. That is, even if **Algorithm 1** yields a stable matching subcarrier assignment solution, as soon as the subcarriers are assigned to the MBS users, the appearance of intra-cell interference terms may not necessary preserve the stability of the subcarrier assignment solution—even after solving problem **GEE-PA-Stage-1**—as it mainly aims at maximizing the GEE for the MBS users, for a fixed subcarrier assignment. A similar observation can be made for the SBS-tier. Particularly, the obtained subcarrier assignment for SBS-users may not necessarily be stable after assigning the subcarriers to the SBS-users, which is due to the intra- and inter-cell interference terms, and irrespective of the solution of problem **GEE-PA-Stage-2**.

Based on the above, it essential to ensure stability of all users and subcarriers after subcarrier assignment and power allocation, and without violating the minimum rate constraints, maximum transmit energy constraint per subcarrier, or degrading the network global energy-efficiency. In this work, the notion of two-sided exchange-stability is considered [16], which is detailed as follows.

Definition 12 (Swap Matching): Given a matching $\overline{\mathcal{M}}$, then users U_i and U_j (for $i \neq j$) swap their subcarrier assignments, while keeping the other user and subcarrier assignments unchanged, yielding the matching

$$\overline{\overline{\mathcal{M}}} = \left\{\overline{\mathcal{M}} \setminus \left\{\left(U_i, \overline{\mathcal{M}}\left(U_i\right)\right), \left(U_j, \overline{\mathcal{M}}\left(U_j\right)\right)\right\}\right\} \cup \left\{\left(U_i, \overline{\mathcal{M}}\left(U_j\right)\right), \left(U_j, \overline{\mathcal{M}}\left(U_i\right)\right)\right\}, \tag{37}$$

$$\bar{\bar{R}}_{m,i}\left(\mathbf{Q}, \bar{\mathbf{x}}\right) = \sum_{SC_k \in \mathcal{SC}} \alpha^k_{m,i} \left(Q^k_{m,i} + \log_2\left(\bar{x}^k_{m,i} |h^k_{m,i}|^2\right) - \log_2\left(|h^k_{m,i}|^2 \left(\sum_{\substack{U_{i'} \in \mathcal{U}_m \\ i' > i}} \bar{x}^k_{m,i'} 2^{Q^k_{m,i'}} \right) + \sum_{\substack{BS_{m'} \in \mathcal{B} \\ m' \neq m}} |h^k_{m',i}|^2 \left(\sum_{U_{i'} \in \mathcal{U}_{m'}} \bar{x}^k_{m',i'} 2^{Q^k_{m',i'}} \right) + N_0 \right) \right) + \beta^k_{m,i}. \tag{35}$$

which involves swapping the allocated transmit energy to users U_i and U_j due to the swapped subcarriers.

For notational convenience, let $\bar{\bar{x}}$ and $\bar{\bar{\mathbf{E}}}$ denote the updated subcarrier assignment due to the obtained matching $\overline{\overline{\mathcal{M}}}$.

Definition 13 (Swap-Blocking Pair): A pair of subcarriers (SC_k, SC_l), for $k \neq l$ form a swap-blocking pair for matching $\overline{\mathcal{M}}$ iff:

(1) $\forall U_i \in \mathcal{U}_m, \forall BS_m \in \mathcal{B}, R_{m,i}\left(\bar{\bar{\mathbf{E}}}, \bar{\bar{x}}\right) \geq R_{m,i}\left(\bar{\mathbf{E}}, \bar{x}\right)$, and $\exists U_i \in \mathcal{U}_m$, for any $BS_m \in \mathcal{B}, R_{m,i}\left(\bar{\bar{\mathbf{E}}}, \bar{\bar{x}}\right) > R_{m,i}\left(\bar{\mathbf{E}}, \bar{x}\right)$.

(2) $\boldsymbol{GEE}\left(\bar{\bar{\mathbf{E}}}, \bar{\bar{\mathbf{x}}}\right) > \boldsymbol{GEE}\left(\bar{\mathbf{E}}, \bar{\mathbf{x}}\right)$.

(3) $\sum_{BS_m \in \mathcal{B}} \sum_{U_i \in \mathcal{U}_m} \bar{\bar{x}}^k_{m,i} \bar{\bar{E}}^k_{m,i} \leq E^{\max}$, and $\sum_{BS_m \in \mathcal{B}} \sum_{U_i \in \mathcal{U}_m} \bar{\bar{x}}^l_{m,i} \bar{\bar{E}}^l_{m,i} \leq E^{\max}$.

(4) $\sum_{U_i \in \mathcal{U}_m} \sum_{SC_k \in \mathcal{SC}} \bar{\bar{x}}^k_{m,i} \bar{\bar{E}}^k_{m,i} + E_{C,m} \leq \mathcal{E}_m, \forall BS_m \in \mathcal{B}$.

Specifically, if two users are to initiate the swap of a pair of subcarriers, then the rates of all users should not be decreased after the swap, and at least one user strictly improves its rate. Additionally, the swap matching must strictly improve the network GEE, without violating the total transmit energy constraint over the swapped subcarriers, or the total energy consumption constraint of each base-station after the swap.

Remark 18: The elimination of a swap-blocking pair does not alter the network total energy consumption. That is, $\sum_{BS_m \in \mathcal{B}} \sum_{U_i \in \mathcal{U}_m} \sum_{SC_k \in \mathcal{SC}} \bar{\bar{x}}^k_{m,i} \bar{\bar{E}}^k_{m,i} + E_{C,m} = \sum_{BS_m \in \mathcal{B}} \sum_{U_i \in \mathcal{U}_m} \sum_{SC_k \in \mathcal{SC}} \bar{x}^k_{m,i} \bar{E}^k_{m,i} + E_{C,m}$, which implies that the total energy consumption remains constant during a swap-operation.

Definition 14 (Two-Sided Exchange-Stability): A matching $\overline{\overline{\mathcal{M}}}$ is said to be *two-sided exchange-stable* if it does not contain any swap-blocking pairs[11].

A. ALGORITHM DESCRIPTION

Initially, for a given matching $\overline{\mathcal{M}}$ obtained via **Algorithm 1** over the two stages, each user searches for another user, and checks if a pair of subcarriers forms a swap-blocking pair. If a swap-blocking pair is found, then a swap-operation is performed, and the matching is updated to $\overline{\overline{\mathcal{M}}}$. This process repeats until convergence, as given in Algorithm 5.

B. PROPERTIES

1) CONVERGENCE:

Lemma 6: **Algorithm 4** converges to a matching $\overline{\overline{\mathcal{M}}}$ in a finite number of iterations.

Proof: Refer to Appendix F. ■

2) COMPLEXITY:

Lemma 7: **Algorithm 4** has a worst-case polynomial-time complexity of $\mathcal{O}\left(K^2\right)$ per user pair.

Proof: Refer to Appendix G. ■

It is noteworthy that **Algorithm 4** does not ensure stability just yet, as it only eliminates swap-blocking pairs, and updates the resulting user-subcarrier assignment. More importantly, for the updated matching, GEE-maximizing power allocation is yet to take place, which in turn may result in further swap-blocking pairs. However, by repeatedly executing **Algorithm 4** and updating the power allocation, a two-sided exchange-stable matching can be obtained, as will be detailed in the following section.

[11] This kind of stability is also known as pairwise stability [16].

Algorithm 4 Swap Matching

Input: Matching $\overline{\mathcal{M}}$

1: FOR each user pair $\left(U_i, U_j\right) \in \mathcal{U}$
2: IF the pair (SC_k, SC_l) forms a swap-blocking pair
3: Perform a swap-operation, and update matching to $\overline{\overline{\mathcal{M}}}$;
4: END IF
5: END FOR

Output: Updated matching $\overline{\overline{\mathcal{M}}}$.

VII. PROPOSED SOLUTION PROCEDURE

In this section, the proposed solution procedure for joint subcarrier assignment and global energy-efficient power allocation (SP-J-SA-GEE-PA) is devised.

A. DESCRIPTION

The **SP-J-SA-GEE-PA** encompasses two stages, where in the first stage, the preference lists of all MBS users (in $\mathcal{U}_0$) and subcarriers are constructed based on a feasible transmit energy matrix, and then **Algorithm 1** is utilized to obtain the initial subcarrier assignment matching solution for the MBS users (i.e. $\bar{\mathbf{x}}^M = \overline{\mathcal{M}}^M$). Based on the obtained subcarrier assignment, **Algorithm 3** is executed to determine the GEE-maximizing power allocation solution $\bar{\mathbf{E}}^M$ for the MBS users. In the second stage, the preference lists of all SBS users and subcarriers are constructed based on a feasible transmit energy matrix for the SBS users, and then the subcarrier assignment $\bar{\mathbf{x}}^S = \overline{\mathcal{M}}^S$ for the SBS users is similarly obtained by executing **Algorithm 1**. After that, **Algorithm 3** is executed to compute the network GEE-maximizing power allocation solution $\bar{\mathbf{E}}$. To enforce stability, **Algorithm 4** is repeatedly executed to eliminate any subcarrier swap-blocking pairs, and update the user-subcarrier assignment matching to $\overline{\overline{\mathcal{M}}}$, while optimizing the network GEE via **Algorithm 3**. This process repeats until convergence to the subcarrier assignment and GEE-maximizing power allocation solutions $\mathbf{x}^*$ and $\mathbf{E}^*$, respectively, and as outlined in Algorithm 5.

Lemma 8: **Algorithm 5** converges to a two-sided exchange-stable matching $\mathbf{x}^*$ in a finite number of iterations, and the solution $(\mathbf{E}^*, \mathbf{x}^*)$ satisfies the KKT conditions.

Proof: Refer to Appendix H. ■

B. DISCUSSION

The formulated **J-SA-GEE-PA** problem is excessively computationally-expensive, as per **Remarks 7** and **8**, especially in dense HetNets. More importantly, it cannot be solved

Algorithm 5 Solution Procedure for Joint Subcarrier Assignment and Global Energy-Efficient Power Allocation (SP-J-SA-GEE-PA)

Input: Users set $\mathcal{U}$ and subcarriers set $\mathcal{SC}$.

Stage 1:

1: Construct preference lists $\mathcal{P}_{U_i}$ and $\mathcal{P}_{SC_k}$, $\forall U_i \in \mathcal{U}_0$, and $\forall SC_k \in \mathcal{SC}$;
2: Determine $\bar{\mathbf{x}}^M = \overline{\mathcal{M}}^M$ via **Algorithm 1**;
3: Solve problem **GEE-PA-Stage-1** via **Algorithm 3** to get $\bar{E}^M$ for fixed $\bar{\mathbf{x}}^M$;

Stage 2:

4: Construct preference lists $\mathcal{P}_{U_i}$ and $\mathcal{P}_{SC_k}$, $\forall U_i \in \mathcal{U}_m$ ($\forall m \geq 1$), and $\forall SC_k \in \mathcal{SC}$;
5: Determine $\bar{\mathbf{x}}^S = \overline{\mathcal{M}}^S$ via **Algorithm 1**;
6: Solve problem **GEE-PA-Stage-2** via **Algorithm 3** to get $\bar{E}$ for fixed $\bar{\mathbf{x}} = \left(\bar{\mathbf{x}}^M, \bar{\mathbf{x}}^S\right)$;
7: WHILE (a swap-blocking pair exists)
8: Execute **Algorithm 4** to eliminate swap-blocking pairs and update matching to $\overline{\overline{\mathcal{M}}}$;
9: Set $\bar{\bar{\mathbf{x}}}^* = \overline{\overline{\mathcal{M}}}$;
10: Solve problem **GEE-PA-Stage-2** via **Algorithm 3** to get $\bar{\bar{E}}^*$ for fixed $\bar{\bar{\mathbf{x}}}^*$;
11: END WHILE

Output: $\mathbf{x}^* = \bar{\bar{\mathbf{x}}}^*$ and $\mathbf{E}^* = \bar{\bar{\mathbf{E}}}^*$.

accurately due to the excessive computational-delay, and even state-of-the-art optimization packages can at best compute near-optimal approximate solutions [14]. Remarkably, problem **J-SA-GEE-PA** does not necessarily ensure stable subcarrier assignment, although if solved optimally, it yields the global optimal energy-efficient solution. This is because it aims at obtaining the global optimal joint subcarrier assignment and GEE solution without any bearing on the stability of each (user, subcarrier) pair. That is, a certain (user, subcarrier) pair may be formed in the solution of problem **J-SA-GEE-PA**; however, such pair may be excluded from the subcarrier assignment solution of the **DA** or swap-matching algorithms to ensure stability. Thus, the **SP-J-SA-GEE-PA** algorithm yields a tradeoff between complexity, optimality and stability. To see this, note that the proposed **DA** and swap-matching algorithms have a worst-case polynomial-time complexity, as stated in subsections IV-C.3 and VI-B.2. Moreover, the solution of problems **GEE-PA-Stage-1** and **GEE-PA-Stage-2** requires fewer numbers of decision variables and constraints in comparison to problem **J-SA-GEE-PA**, as per **Remarks 8**, **13**, and **17**. On top of that, the aforementioned two GEE-PA problems can be solved optimally and with minimal computational-complexity via **Algorithm 3**. However, such low-complexity comes at the expense of some global sub-optimality. This is due to the fact that the **SP-J-SA-GEE-PA** algorithm decouples problem **J-SA-GEE-PA** into two sub-problems and solves them over two stages, which does not necessarily ensure global optimality, due to the enforced stability.

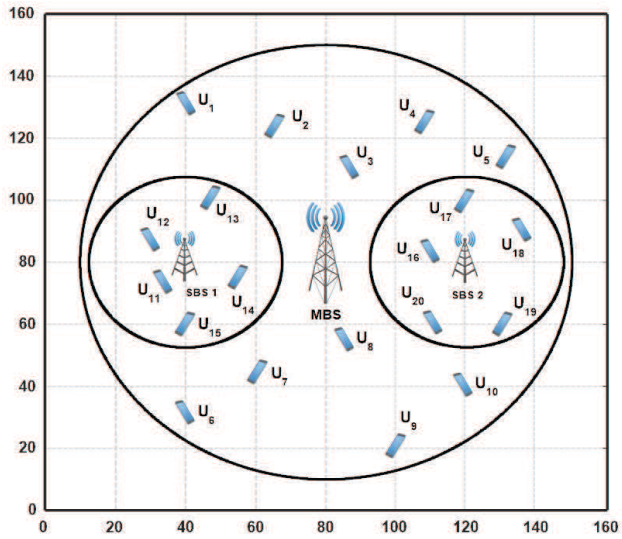

FIGURE 2. Simulated Network Topology.

Lastly, it should be noted that the proposed **SP-J-SA-GEE-PA** algorithm requires a centralized controller, which gathers channel state and energy-harvesting information from all base-stations, and then communicates the subcarrier assignment and power allocation decisions to all base-stations. Specifically, the base-stations may be connected to the central unit via high-capacity backhaul links, while ensuring energy-efficient communications [33], [34].

VIII. SIMULATION RESULTS

In this section, the proposed **SP-J-SA-GEE-PA** scheme is evaluated[12]. The simulations assume a total of $M = 3$ base-stations (i.e. a MBS, and 2 SBSs), as illustrated in Fig. 2. In addition, there is a total of $N = 20$ users, where the MBS includes users $\mathcal{U}_0 = \{U_1, \ldots, U_{10}\}$ (i.e. 10 users), $\mathcal{U}_1 = \{U_{11}, \ldots, U_{15}\}$, and $\mathcal{U}_2 = \{U_{16}, \ldots, U_{20}\}$ (i.e. each SBS has 5 users). Moreover, there is a total of $K = 8$ subcarriers, which can be utilized by all users within all base-stations[13]. The total transmit energy per subcarrier is set to $E^{\max} = 0.5$ J. The noise variance is set to $N_0 = 10^{-8}$ J, while the path-loss exponent is set to $\nu = 3$. The target minimum rate per MBS user is set to $\mathbb{R}^M_{\min} = 2.5$ bits/s/Hz, and $\mathbb{R}^S_{\min} = 1.5$ bits/s/Hz for the SBS users. The maximum harvested energy per time-slot at each base-station is set to $\mathcal{E}^{\max}_m = 3$, 1.5, and 1.5 J, while the fixed transceiver energy consumption $E_{C,m} = 0.01$, 0.005, and 0.005 J, for $m = 0, 1, 2$. The battery capacity is set to $B^{\max}_m = 10$, 5, and 5 J, for $m = 0, 1, 2$. The simulations are averaged over 10^3 random network instances, each of 10 time-slots (i.e. $\tau = 1, \ldots, 10$), with randomly generated channel coefficients that remain constant during each network instance, but vary from one network instance

[12]The tolerance for **Algorithms 2** and **3** is set to $\epsilon = 0.001$ (i.e. optimal within three decimal places).

[13]Note that the number of users in each tier is greater than the number of available subcarriers.

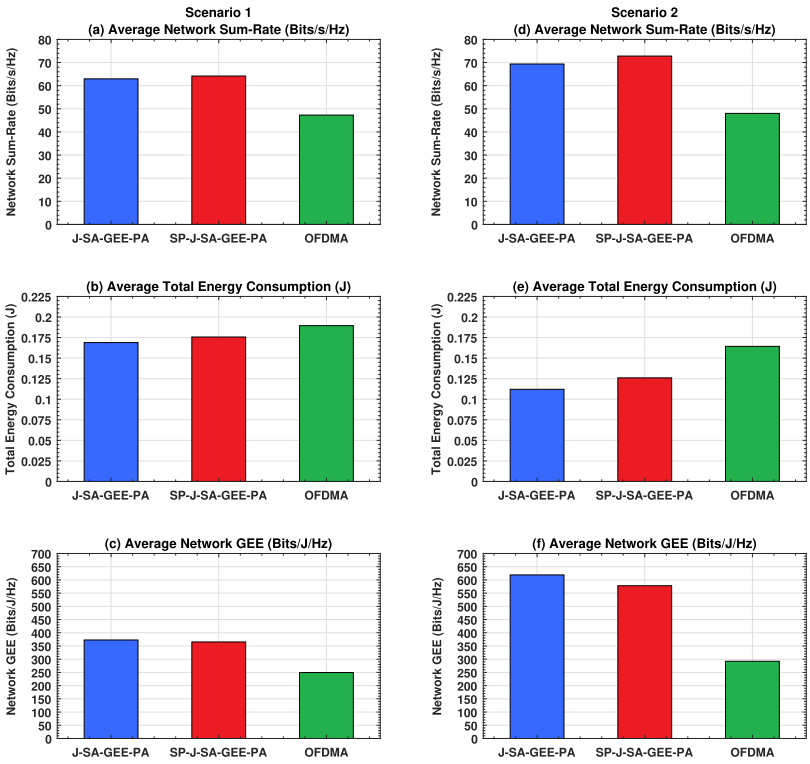

FIGURE 3. Scenario 1: (a) Average Network Sum-Rate (Bits/s/Hz), (b) Average Total Energy Consumption (J), and (c) Average Network GEE (Bits/J/Hz) Scenario 2: (d) Average Network Sum-Rate (Bits/s/Hz), (e) Average Total Energy Consumption (J), and (f) Average Network GEE (Bits/J/Hz).

to another. Moreover, the energy arrivals $\mathcal{E}_m^\tau$ at each time-slot τ are randomly generated, as discussed in subsection II-B.

In addition, the proposed **SP-J-SA-GEE-PA** scheme is compared to the **J-SA-GEE-PA** scheme and **OFDMA**[14]. Moreover, the following scenarios are considered:

Scenario 1: $\xi_k^M = \xi_k^S = 2, \forall SC_k \in \mathcal{SC}$, and $\zeta_i^M = \zeta_i^S = 2, \forall U_i \in \mathcal{U}_m$, and $\forall BS_m \in \mathcal{B}$.

Scenario 2: $\xi_k^M = \xi_k^S = 3, \forall SC_k \in \mathcal{SC}$, and $\zeta_i^M = \zeta_i^S = 3, \forall U_i \in \mathcal{U}_m$, and $\forall BS_m \in \mathcal{B}$.

Particularly, the above scenarios aim at investigating the effect of increasing the number of assignable users per subcarrier as well as the number of subcarriers assignable to each user on the network global energy-efficiency. However, it should be noted that in **OFDMA**, $\xi_k^M = \xi_k^S = 1, \forall SC_k \in \mathcal{SC}$, under both scenarios. That is, in the **OFDMA** scheme, a subcarrier can be assigned to at most one user in each tier, but each user can be assigned multiple subcarriers[15].

Under **Scenario 1**, it is evident from Fig. 3a that the **SP-J-SA-GEE-PA** scheme yields slightly higher average network sum-rate than the **J-SA-GEE-PA** scheme; however, at the expense of slightly higher average energy consumption (see Fig. 3b). In comparison to **OFDMA**, the **SP-J-SA-GEE-PA** scheme yields higher average network sum-rate, but with less total energy consumption. More importantly, the **SP-J-SA-GEE-PA** scheme yields slightly less (but comparable) network GEE to the **J-SA-GEE-PA** scheme, and significantly outperforms **OFDMA**, as shown in Fig. 3c[16]. Thus, it would be expected that the average residual energy at the base-stations to be slightly less under the **SP-J-SA-GEE-PA** scheme than the **J-SA-GEE-PA** scheme, but significantly higher than **OFDMA**. The minor sub-optimality of the **SP-J-SA-GEE-PA** scheme in comparison to the **J-SA-GEE-PA** scheme is attributed to the fact that in order to ensure stability under the **SP-J-SA-GEE-PA** scheme, (user, subcarrier) and/or swap-blocking pairs are eliminated, which may have been assigned under the **J-SA-GEE-PA** scheme to yield the global optimal GEE solution, as stated in subsection VII-B. Generally speaking, allowing multiple users—in each tier—to share a subcarrier (via NOMA) improves the network GEE, as opposed to orthogonal multiple-access (i.e. via **OFDMA**). Similar observations can be made for **Scenario 2**, as illustrated in Figs. 3d—3f. Remarkably, under **Scenario 2**, the

[14] All optimization problems are solved via MIDACO [35], with tolerance set to 0.001.

[15] To the best of our knowledge, no prior work has considered similar problem formulation and constraints to our work, and thus comparison to other schemes would not be possible. In addition, our algorithmic solutions are applicable to arbitrary numbers of users, subcarriers, and SBSs, and network topologies.

[16] Recall that the network GEE is proportional to the network sum-rate R_T but inversely proportional to the total energy consumption E_T. Moreover, the rate function is logarithmic in the allocated transmit energy, while the total energy consumption is linear in the transmit energy. That is, R_T increases at a slower rate than E_T.

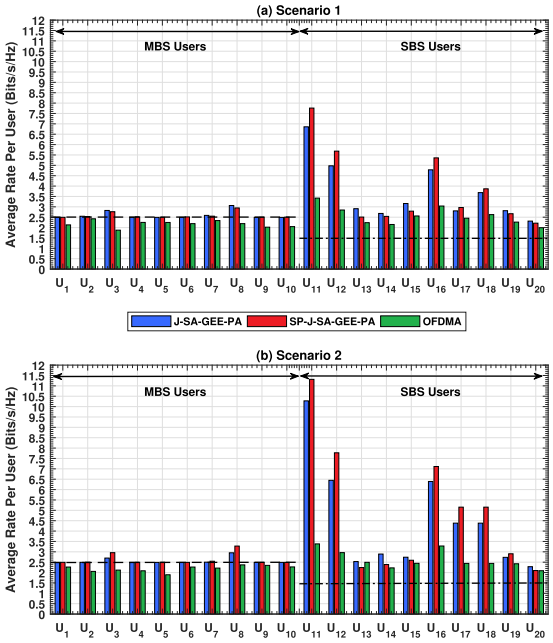

FIGURE 4. Average Rate Per User (Bits/s/Hz): (a) Scenario 1, and (b) Scenario 2.

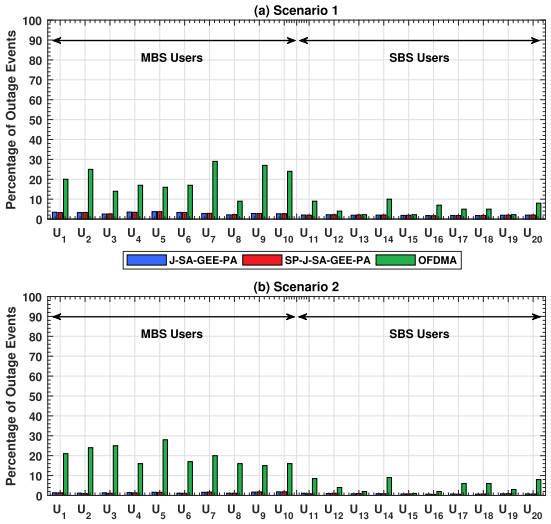

FIGURE 5. Percentage of Outage Events: (a) Scenario 1, and (b) Scenario 2.

J-SA-GEE-PA and **SP-J-SA-GEE-PA** schemes yield higher average network sum-rate, and less energy consumption than in **Scenario 1**. In turn, higher average network GEE is achieved under **Scenario 2** in comparison to **Scenario 1**. This is due to the increase in the number of subcarriers assignable to each user in each tier as well as the increase in the number of users that can share a subcarrier[17]. As for **OFDMA**, that the average network sum-rate under both scenarios is almost the same (with negligible improvement in **Scenario 2**), despite the increase in the number of subcarriers assignable to each user in each tier. This is because each subcarrier can be assigned to at most one user, and in each tier, the number of users exceeds the number of subcarriers. In other words, under both scenarios, not all users can be assigned to subcarriers, which in turn does not significantly affect the average network sum-rate. However, under **Scenario 2**, the average energy consumption is lower than in **Scenario 1**, as each user in each tier has larger subsets of assignable subcarriers in order to achieve its minimum rate requirement. This in turn results in slightly improved average network GEE for **OFDMA** in **Scenario 2**.

Fig. 4a illustrates the average rate per user under **Scenario 1**, where it is evident that all MBS users under the **SP-J-SA-GEE-PA** and **J-SA-GEE-PA** schemes meet the target minimum rate of $\mathbb{R}^{M}_{\min} = 2.5$ bits/s/Hz; however, this is not the case for **OFDMA**. This is because each subcarrier can be assigned to at most one user, and the number of users exceeds the number of subcarriers. Contrarily, all SBS users under all schemes significantly exceed their minimum rate requirement of $\mathbb{R}^{S}_{\min} = 1.5$ bits/s/Hz. This is attributed to their locations being relatively closer to their respective base-stations than the MBS users. It can also be seen that for the MBS users, U_8 achieves the highest average rate under the **SP-J-SA-GEE-PA** and **J-SA-GEE-PA** schemes, which is due to its location being relatively closer to the MBS than the other users. This also applies to users U_{11} and U_{16} in SBSs 1, and 2, respectively. In Fig. 4b, the average rate per user under **Scenario 2** is shown. Similar observations to the MBS users in **Scenario 1** can be made. However, for SBS users U_{11}, U_{12}, U_{16}, U_{17} and U_{18}, their average rate values have significantly improved under the **SP-J-SA-GEE-PA** and **J-SA-GEE-PA** schemes, which is mainly due to the increase in the number of users that can be assigned to each subcarrier and vice versa. This has the effect of improving the network sum-rate and also reducing the energy consumption, which translates to improved network GEE, as shown in Fig. 3f.

In Fig. 5a, the percentage of outage events under **Scenario 1** is depicted[18]. It is evident that the **SP-J-SA-GEE-PA** and **J-SA-GEE-PA** schemes yield lower percentages of outage events than **OFDMA**, especially for the MBS users. Moreover, under **OFDMA**, the SBS users achieve lower percentages of outage events than the MBS users, which is mainly due to their minimum rate requirement being less than MBS users, as well as the fact that they are relatively closer to their respective base-stations (i.e. less path-loss). As for **Scenario 2**, one can see that the percentages of outage events under the **SP-J-SA-GEE-PA** and **J-SA-GEE-PA** schemes have decreased, which is due to the increase in the number of users that can be assigned to each subcarrier, and vice versa. However, this is not the case for **OFDMA**.

[17] Despite the improvement in the network GEE due to the increase in the number of users assignable to each subcarrier, this increases the SIC receiver complexity, as per **Remark 5**, which poses a tradeoff.

[18] An outage occurs when a user cannot satisfy its minimum rate requirement, which may be caused by not being assigned a sufficient number of subcarriers, or insufficient harvested energy at the base-station.

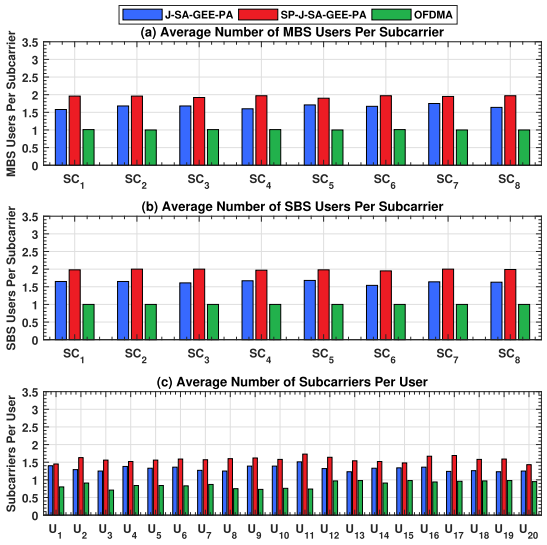

FIGURE 6. Scenario 1: (a) Average Number of MBS Users Per Subcarrier, (b) Average Number of SBS Users Per Subcarrier, and (c) Average Number of Subcarriers Per User.

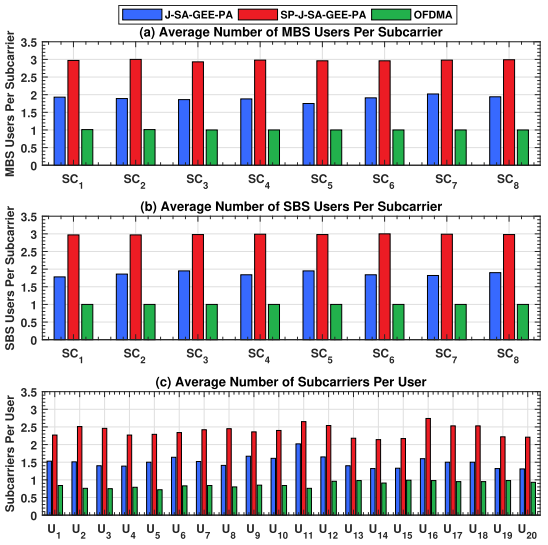

FIGURE 7. Scenario 2: (a) Average Number of MBS Users Per Subcarrier, (b) Average Number of SBS Users Per Subcarrier, and (c) Average Number of Subcarriers Per User.

In Figs. 6a and 6b, it can be seen that the average number of MBS and SBS users per subcarrier—in **Scenario 1**—is at most two for the **SP-J-SA-GEE-PA** and **J-SA-GEE-PA** schemes, with the **SP-J-SA-GEE-PA** scheme assigning slightly higher average number of users to each subcarrier to ensure stability and maximize the GEE. This is also a direct result of using the extended max-min criterion to create the preference lists of the users and subcarriers, as per **Remark 12**. On the other hand, it can be verified that all subcarriers are assigned to exactly one user in each tier by **OFDMA**, which also implies 100% subcarriers assignment to the users, since the number of users exceeds the number of subcarriers in each tier. Fig. 6c shows that the average number of subcarriers per user is less than two for the **SP-J-SA-GEE-PA** and **J-SA-GEE-PA** schemes, with the average number of subcarriers per user in the former scheme being slightly higher than the latter. Additionally, for **OFDMA**, the average number of subcarriers per user does not exceed one, although each user can be assigned up to two subcarriers. However, since each subcarrier can be assigned to at most one user in each tier, and the number of users exceeds the number of subcarriers, then each user is assigned—on average—not more than one subcarrier. Similar observations can be made in Figs. 7a—7c for **Scenario 2**; however, with the difference in that the subcarriers are assigned at most three users in the MBS- and SBS-tiers, under the **SP-J-SA-GEE-PA** scheme. Moreover, the average number of assigned subcarriers per user under the **SP-J-SA-GEE-PA** scheme does not exceed three. Generally speaking, the average number of users (subcarriers) per subcarrier (user) in **Scenario 2** for the **SP-J-SA-GEE-PA** and **J-SA-GEE-PA** schemes is higher than in **Scenario 1**, as would be expected, which is not the case for **OFDMA**.

Fig. 8a illustrates the average number of iterations required by the **DA** algorithm (i.e. **Algorithm 1**) to find a stable matching solution under both scenarios. In **Scenario 1**, it is clear that the average number of iterations in Stage 1 (i.e. MBS users) is less than 10, and in Stage 2 (i.e. SBS users) is less than 9. Similar observations are made for **Scenario 2**. Remarkably, the average number of iterations of **Algorithm 1** is less in **Scenario 2** than in **Scenario 1**. This is because with the increase in the number of users assignable to each subcarrier (and vice versa), it is relatively easier to find a stable matching (subcarrier assignment) solution. Moreover, it is noticed under both scenarios that the average number of iterations in the MBS-tier is greater than that in the SBS-tier. This is due to the fact that the rate requirement for the SBS users is less than that for the MBS users, which implies relatively larger preference lists of acceptable SBS users and subcarriers, and hence it is less complex to find a stable subcarrier assignment solution in the SBS-tier. Fig. 8b shows the average number of iterations of **Algorithm 2**, where in **Scenario 1**, less than 5 iterations are required in Stage 1, and less than 7 iterations are required for Stage 2. In general, Stage 2 requires slightly more iterations than Stage 1, as problem **R-GEE-PA-Stage-2** involves a larger number of decision variables and constraints than problem **R-GEE-PA-Stage-1**, as it incorporates all network users, as opposed to problem **R-GEE-PA-Stage-1**, which involves only the MBS users (see **Remarks 13** and **17**). Similar observations can be made to **Scenario 2**; however, it can be seen that the average number of iterations are marginally less than in **Scenario 1**. This is because in **Scenario 2**, the number of users that can be assigned to each subcarrier (and vice versa) is greater than that in **Scenario 1** (i.e. a larger feasible region), which implies that problems **R-GEE-PA-Stage-1** and **R-GEE-PA-Stage-2** can be solved relatively easier than in **Scenario 1**. Similar observations and justifications can also be applied to **Algorithm 3** in **Scenarios 1** and **2**, as shown in Fig. 8c.

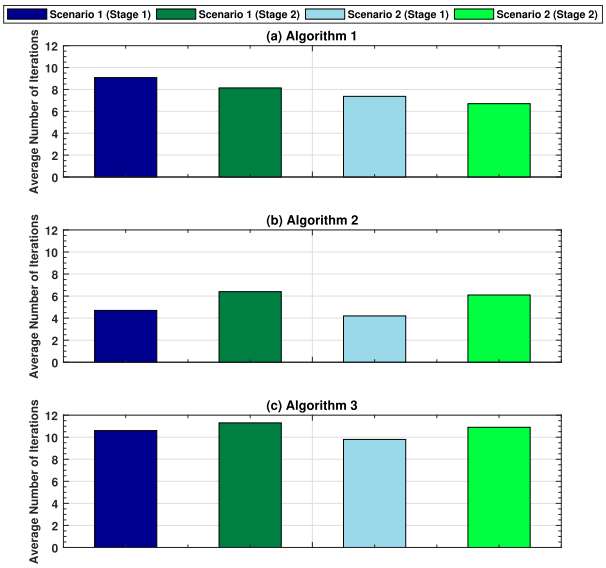

FIGURE 8. Average Number of Iterations: (a) Algorithm 1, (b) Algorithm 2, and (c) Algorithm 3.

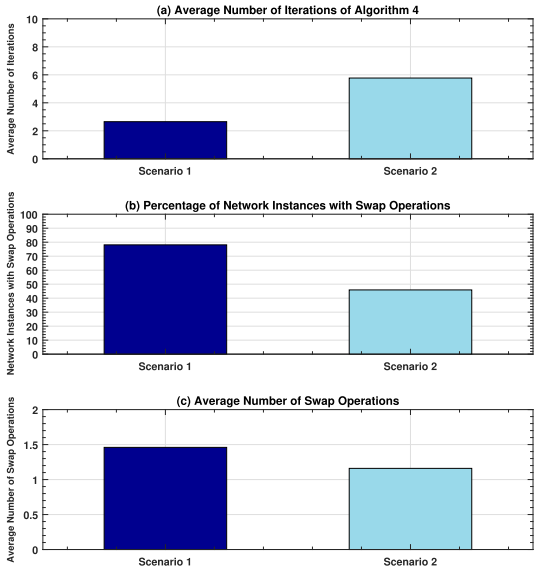

FIGURE 9. (a) Average Number of Iterations of Algorithm 4, (b) Percentage of Network Instances with Swap Operations, and (c) Average Number of Swap Operations.

Fig. 9a depicts the average number of iterations of **Algorithm 4** in **Scenarios 1** and **2**. Specifically, one can see that **Scenario 2** involves higher number of iterations–on average–than **Scenario 1**, which due to the increase in the number of users that can be assigned to each subcarrier (and vice versa). That is, a greater number of subcarriers pair must be checked if they form swap-blocking pairs among all user pairs. Nevertheless, the complexity of **Algorithm 4** per user pair is significantly less than $\mathcal{O}\left(K^2\right)$ under both scenarios (see **Lemma 7**), which is due to the quota on the number of users and subcarriers than can be assigned. In Fig. 9b, the percentage of network instances with swaps is illustrated for **Scenarios 1** and **2**. Specifically, one can see that in **Scenario 1** (**Scenario 2**), about 78% (46%) of the simulated network instances involve at least one swap operation. Notably, there are fewer instances with swap operations in **Scenario 2** than in **Scenario 1**. This is due to the increase in the number of users that are assigned to each subcarrier (and vice versa), and thus it is more difficult to find a subcarriers swap-blocking pair that satisfies the conditions given in **Definition 13**. This also implies that the user-subcarrier assignment is two-sided exchange-stable more often in **Scenario 2** than in **Scenario 1**. In other words, increasing the quota of users and subcarriers improves the network stability, as users are less often tempted to swap their assigned subcarriers. Fig. 9c illustrates the average number swap operations in **Scenarios 1** and **2**, where it is evident that **Scenario 2** involves—on average—slightly less number of iterations, in agreement with the observations made in Fig. 9b.

Based on the results presented in Figs. 8 and 9, and the discussion given in subsection VII-B, it is evident that the proposed two-stage solution procedure (in **Algorithm 5**) can be efficiently executed (i.e. with minimal computational-complexity) to obtain the joint subcarrier assignment and global energy-efficiency maximizing power allocation solution, which has also been shown to be comparable to the **J-SA-GEE-PA** scheme, and superior to **OFDMA**.

IX. CONCLUSION

This paper has studied the problem of joint subcarrier assignment and global energy-efficient power allocation for energy-harvesting two-tier downlink NOMA HetNets. However, the J-SA-GEE-PA problem has been shown to be computationally-prohibitive, and thus has been split into two sub-problems. For the first sub-problem, the subcarrier assignment problem has been modeled as a many-to-many matching problem, while for the second sub-problem, the global energy-efficient power allocation has been solved optimally via a low-complexity algorithm. After that, an iterative solution procedure has been proposed to efficiently solve the J-SA-GEE-PA problem over two stages, while ensuring two-sided exchange-stability. Simulation results have been presented to validate the proposed solution procedure, which has been shown to yield comparable network energy-efficiency to the J-SA-GEE-PA scheme (solved via a global optimization package), and superior to that of OFDMA; however, with lower computational-complexity.

APPENDIX A
LEMMA 1

Proof: Since the preference lists of the users and subcarriers are constructed based on the extended max-min criterion, which implies substitutable preferences (as per **Remark 10**), then the set of stable matching solutions is not empty [22], [24]. Thus, at least one stable matching solution exists. ■

APPENDIX B
LEMMA 2

Proof: This is a direct result of the fact that no user proposes twice to the same subcarrier. Moreover, the algorithm terminates when there are no more rejections, and thus each subcarrier is assigned to the users on its waiting list in the last iteration. ■

APPENDIX C
LEMMA 3

Proof: The aim is to show that for any other matching $\widetilde{\mathcal{M}}$, the resulting stable matching solution $\overline{\mathcal{M}}$ is strictly preferred by each user to $\widetilde{\mathcal{M}}$. Now, assume that some user $U_i \in \mathcal{U}_m$ and some subcarrier $SC_k \in \mathcal{SC}$ are *assignable* to each other (i.e. acceptable to each other) in some matching instance if they can be matched under some stable assignment. In the **DA** algorithm, one must show that no user is ever rejected by an assignable subcarrier, and thus the $\overline{\mathcal{M}}$ stable matching solution is obtained by assigning each user to its most preferred subcarriers. Then, $\overline{\mathcal{M}}$ must be the unique.

The proof proceeds using contradiction. Specifically, assume that there exists some user that was previously rejected by a subcarrier. Let $\ell \geq 1$ be the first step when at least one user U_i was rejected by its assignable subcarrier SC_k[19]. Now, if SC_k rejects user U_i because it is unacceptable, then SC_k is by definition not assignable to U_i. However, if U_i is acceptable to SC_k, then SC_k rejects U_i if it has a more preferred user on its waiting list. By recalling the extended max-min criterion, there must be ξ_k users that are better than U_i on its waiting list at the end of Step ℓ. For convenience, let the set of ξ_k such users be denoted by $\mathcal{W}(SC_k)$, which will be used to show that SC_k is not assignable to U_i. Intuitively, any other user $U_j \in \mathcal{W}(SC_k)$ (for $U_j \neq U_i$) must have proposed to SC_k at Step ℓ or before. That is, U_j was not rejected by any subcarrier that is assignable to it before Step ℓ. In turn, there are fewer subcarriers than ζ_j that are assignable to U_j, and simultaneously better than SC_k for U_j. Since, SC_k and U_i have been assumed to be assignable to each other, then there exists some other stable matching $\widetilde{\mathcal{M}}$, such that $U_i \in \widetilde{\mathcal{M}}(SC_k)$. However, since $|\widetilde{\mathcal{M}}(SC_k)| \leq \xi_k$, $|\mathcal{W}(SC_k)| = \xi_k$, $U_i \in \widetilde{\mathcal{M}}(SC_k)$, and $U_i \notin \mathcal{W}(SC_k)$, then $\mathcal{W}(SC_k) \setminus \widetilde{\mathcal{M}}(SC_k)$ is not empty. That is, there exists some other subcarrier $SC_l \in \mathcal{W}(SC_k) \setminus \widetilde{\mathcal{M}}(SC_k)$, for $l \neq k$. Consequently, since there are fewer than ζ_j subcarriers that are assignable to U_j, and are more preferred than SC_k by U_j, then either $|\widetilde{\mathcal{M}}(U_j)| < \zeta_j$, or there exists some other subcarrier $SC_l \in \mathcal{SC}$, where $SC_l \in \widetilde{\mathcal{M}}(U_j)$ and $SC_k \succ_{U_j} SC_l$. Hence, $U_i \in \widetilde{\mathcal{M}}(SC_k)$ with $U_j \succ_{SC_k} U_i$ indicate that $\widetilde{\mathcal{M}}$ is blocked by the pair (U_j, SC_k), which is a contradiction to the stability of $\widetilde{\mathcal{M}}$. Lastly, since the preferences of each user are strict and transitive, and that each user proposes to its most preferred subcarriers, then the resulting stable matching solution $\overline{\mathcal{M}}$ is also unique. ■

[19]This implies that no user was rejected by any of its assignable subcarriers from Step 1 through to Step $\ell - 1$.

APPENDIX D
LEMMA 4

Proof: This is a direct consequence of the fact that when the values of $\alpha_{0,i}^k$ and $\beta_{0,i}^k$ are fixed ($\forall SC_k \in \mathcal{SC}$, and $\forall U_i \in \mathcal{U}_0$), the functions $\bar{R}_T\left(\mathbf{Q}^{(l)}, \bar{\mathbf{x}}^M\right)$ and $\bar{E}_T\left(\mathbf{Q}^{(l)}, \bar{\mathbf{x}}^M\right)$, are respectively concave and convex. In turn, the auxiliary function $\bar{F}\left(\lambda^{(l)}\right)$ is concave for each fixed value of $\lambda^{(l)}$. Now, since the constraints set is convex, and **Algorithm 3** successively solves a maximization problem for each value of $\lambda^{(l)}$, then it is guaranteed to converge to the global optimal solution $\hat{\mathbf{Q}}^M$ of problem **R-GEE-PA-Stage-1** [17], [36]. ■

APPENDIX E
LEMMA 5

Proof: The proof proceeds by noting that in the $(l-1)^{th}$ iteration of **Algorithm 3**, the obtained transmit energy matrix $\hat{\mathbf{E}}^{(l-1)} = 2^{\hat{\mathbf{Q}}^{(l-1)}}$—for fixed values of $\alpha_{0,i}^{k,(l-1)}$ and $\beta_{0,i}^{k,(l-1)}$—maximizes the objective function of problem **R-GEE-PA-Stage-1** (via **Algorithm 2**) subject to the convexified set of constraints of problem **GEE-PA-Stage-1**. According to **Lemma 4**, the global optimal solution of problem **R-GEE-PA-Stage-1** is obtained, and the corresponding objective function value is evaluated as $\widehat{\boldsymbol{GEE}}\left(\hat{\mathbf{E}}^{(l-1)}, \bar{\mathbf{x}}^M\right) = \boldsymbol{GEE}\left(\hat{\mathbf{E}}^{(l-1)}, \bar{\mathbf{x}}^M\right)$, as per (30). Particularly, the equality is due to the updated values of $\alpha_{0,i}^{k,(l)}$ and $\beta_{0,i}^{k,(l)}$, which in turn make the bound in (22) tight [27]. Now, in the l^{th} iteration, $\hat{\mathbf{E}}^{(l)} = 2^{\hat{\mathbf{Q}}^{(l)}}$ maximizes the objective function of problem **R-GEE-PA-Stage-1**, and thus $\widehat{\boldsymbol{GEE}}\left(\hat{\mathbf{E}}^{(l)}, \bar{\mathbf{x}}^M\right) \geq \widehat{\boldsymbol{GEE}}\left(\hat{\mathbf{E}}^{(l-1)}, \bar{\mathbf{x}}^M\right)$. However, since $\widehat{\boldsymbol{GEE}}\left(\hat{\mathbf{E}}^{(l)}, \bar{\mathbf{x}}^M\right)$ is a lower-bounded value of problem **GEE-PA-Stage-1**, then $\boldsymbol{GEE}\left(\hat{\mathbf{E}}^{(l)}, \bar{\mathbf{x}}^M\right) \geq \widehat{\boldsymbol{GEE}}\left(\hat{\mathbf{E}}^{(l)}, \bar{\mathbf{x}}^M\right)$. To sum up, the following inequality holds [37]

$$\begin{aligned} \cdots = \boldsymbol{GEE}\left(\hat{\mathbf{E}}^{(l)}, \bar{\mathbf{x}}^M\right) &\geq \widehat{\boldsymbol{GEE}}\left(\hat{\mathbf{E}}^{(l)}, \bar{\mathbf{x}}^M\right) \\ &\geq \widehat{\boldsymbol{GEE}}\left(\hat{\mathbf{E}}^{(l-1)}, \bar{\mathbf{x}}^M\right) = \boldsymbol{GEE}\left(\hat{\mathbf{E}}^{(l-1)}, \bar{\mathbf{x}}^M\right) \geq \cdots, \end{aligned} \tag{E.1}$$

which implies that $\widehat{\boldsymbol{GEE}}\left(\hat{\mathbf{E}}^{(l)}, \bar{\mathbf{x}}^M\right)$ monotonically increases in each iteration until convergence.

Now, the KKT conditions of problem **R-GEE-PA-Stage-1** can be obtained by formulating the Lagrangian function as follows

$$\begin{aligned} &\mathcal{L}\left(\left\{Q_{0,i}^k\right\}, \{\pi_k\}, \{\rho_{0,i}\}, \left\{\upsilon_{0,i}^k\right\}, \varsigma, \left\{\omega_{0,i}^k\right\}, \left\{\varpi_{0,i}^k\right\}\right) \\ &= \overline{\boldsymbol{GEE}}\left(\mathbf{Q}^M, \bar{\mathbf{x}}^M\right) - \sum_{SC_k \in \mathcal{SC}} \pi_k \left(\sum_{U_i \in \mathcal{U}_0} \bar{x}_{0,i}^k 2^{Q_{0,i}^k} - E^{\max}\right) \\ &\quad + \sum_{U_i \in \mathcal{U}_0} \rho_{0,i}\left(\bar{R}_{0,i}\left(\mathbf{Q}^M, \bar{\mathbf{x}}^M\right) - \mathbb{R}_{\min}^M\right) \\ &\quad + \sum_{i=1}^{|\mathcal{U}_0|-1} \sum_{SC_k \in \mathcal{SC}} \upsilon_{0,i}^k \left(Q_{0,i}^k - Q_{0,i+1}^k\right) \end{aligned}$$

$$
\begin{aligned}
&- \varsigma \left(\sum_{U_i \in \mathcal{U}_0} \sum_{SC_k \in \mathcal{SC}} \bar{x}_{0,i}^k 2^{Q_{0,i}^k} + E_{C,0} - \mathcal{E}_0 \right) \\
&- \sum_{SC_k \in \mathcal{SC}} \sum_{U_i \in \mathcal{U}_0} \omega_{0,i}^k \left(2^{Q_{0,i}^k} - \bar{x}_{0,i}^k E^{\max} \right) \\
&+ \sum_{SC_k \in \mathcal{SC}} \sum_{U_i \in \mathcal{U}_0} \varpi_{0,i}^k 2^{Q_{0,i}^k}, \qquad \text{(E.2)}
\end{aligned}
$$

where $\{\pi_k\}$, $\{\rho_{0,i}\}$, $\left\{\upsilon_{0,i}^k\right\}$, ς, $\left\{\omega_{0,i}^k\right\}$, and $\left\{\varpi_{0,i}^k\right\}$ are the Lagrange multipliers. Thus, the KKT conditions can be obtained by $\frac{\mathcal{L}\left(\left\{Q_{0,i}^k\right\},\{\pi_k\},\{\rho_{0,i}\},\left\{\upsilon_{0,i}^k\right\},\varsigma,\left\{\omega_{0,i}^k\right\},\left\{\varpi_{0,i}^k\right\}\right)}{\partial Q_{0,i}^k}$, yielding (E.3), as shown the bottom of this page, where it should be noted that $\frac{\partial 2^{Q_{0,i}^k}}{\partial Q_{0,i}^k} = \ln(2) 2^{Q_{0,i}^k}$. Specifically, the KKT conditions are obtained as given in (E.3), as shown at the bottom of this page. More importantly, note that $\frac{\partial \overline{\boldsymbol{GEE}}\left(\mathbf{Q}^M, \bar{\mathbf{x}}^M\right)}{\partial Q_{0,i}^k}$ is obtained as in (E.4), as shown at the bottom of this page, where $\overline{\boldsymbol{GEE}}\left(\mathbf{Q}^M, \bar{\mathbf{x}}^M\right)$ is given in (27). Moreover, $\frac{\partial \bar{E}_T\left(\mathbf{Q}^M, \bar{\mathbf{x}}^M\right)}{\partial Q_{0,i}^k} = \ln(2) \bar{x}_{0,i}^k 2^{Q_{0,i}^k}$, and

$$
\begin{aligned}
&\frac{\partial \bar{R}_T\left(\mathbf{Q}^M, \bar{\mathbf{x}}^M\right)}{\partial Q_{0,i}^k} \\
&= \alpha_{0,i}^k - \sum_{j<i} \alpha_{0,j}^k \frac{|h_{0,j}^k|^2 \bar{x}_{0,i}^k 2^{Q_{0,i}^k}}{|h_{0,j}^k|^2 \left(\sum_{\substack{U_{i'} \in \mathcal{U}_0 \\ i'>j}} \bar{x}_{0,i'}^k 2^{Q_{0,i'}^k} \right) + N_0} \\
&= \alpha_{0,i}^k - \sum_{j<i} \alpha_{0,j}^k \frac{|h_{0,j}^k|^2}{\bar{\mathcal{I}}_{0,j}^k + N_0} \bar{x}_{0,i}^k 2^{Q_{0,i}^k}, \qquad \text{(E.6)}
\end{aligned}
$$

$$
\begin{aligned}
&\frac{\partial \overline{\boldsymbol{GEE}}\left(\mathbf{Q}^M, \bar{\mathbf{x}}^M\right)}{\partial Q_{0,i}^k} - \ln(2) \sum_{SC_k \in \mathcal{SC}} \left(\pi_k \sum_{U_i \in \mathcal{U}_0} \bar{x}_{0,i}^k 2^{Q_{0,i}^k} \right) + \frac{\partial}{\partial Q_{0,i}^k} \sum_{U_i \in \mathcal{U}_0} \rho_{0,i} \left(\bar{R}_{0,i}\left(\mathbf{Q}^M, \bar{\mathbf{x}}^M\right) - \mathbb{R}_{\min}^M \right) \\
&\quad + \frac{\partial}{\partial Q_{0,i}^k} \sum_{i=1}^{|\mathcal{U}_0|-1} \sum_{SC_k \in \mathcal{SC}} \upsilon_{0,i}^k \left(Q_{0,i}^k - Q_{0,i+1}^k \right) - \ln(2) \left(\varsigma \sum_{U_i \in \mathcal{U}_0} \sum_{SC_k \in \mathcal{SC}} \bar{x}_{0,i}^k 2^{Q_{0,i}^k} \right) \\
&\quad - \ln(2) \sum_{SC_k \in \mathcal{SC}} \sum_{U_i \in \mathcal{U}_0} \omega_{0,i}^k 2^{Q_{0,i}^k} + \ln(2) \sum_{SC_k \in \mathcal{SC}} \sum_{U_i \in \mathcal{U}_0} \varpi_{0,i}^k 2^{Q_{0,i}^k} = 0. \qquad \text{(E.3)}
\end{aligned}
$$

$$
\begin{aligned}
\pi_k \left(\sum_{U_i \in \mathcal{U}_0} \bar{x}_{0,i}^k 2^{Q_{0,i}^k} - E^{\max} \right) &= 0, \quad \forall SC_k \in \mathcal{SC}, \\
\rho_{0,i} \left(\bar{R}_{0,i}\left(\mathbf{Q}^M, \bar{\mathbf{x}}^M\right) - \mathbb{R}_{\min}^M \right) &= 0, \quad \forall U_i \in \mathcal{U}_0, \\
\upsilon_{0,i}^k \left(Q_{0,i}^k - Q_{0,i+1}^k \right) &= 0, \quad \forall i = 1, \ldots, |\mathcal{U}_0| - 1, \forall SC_k \in \mathcal{SC}, \\
\varsigma \left(\sum_{U_i \in \mathcal{U}_0} \sum_{SC_k \in \mathcal{SC}} \bar{x}_{0,i}^k 2^{Q_{0,i}^k} + E_{C,0} - \mathcal{E}_0 \right) &= 0, \\
\omega_{0,i}^k \left(2^{Q_{0,i}^k} - \bar{x}_{0,i}^k E^{\max} \right) &= 0, \quad \forall SC_k \in \mathcal{SC}, \forall U_i \in \mathcal{U}_0, \\
\varpi_{0,i}^k 2^{Q_{0,i}^k} &= 0, \quad \forall SC_k \in \mathcal{SC}, \forall U_i \in \mathcal{U}_0, \\
\sum_{U_i \in \mathcal{U}_0} \bar{x}_{0,i}^k 2^{Q_{0,i}^k} &\le E^{\max}, \quad \forall SC_k \in \mathcal{SC}, \\
\bar{R}_{0,i}\left(\mathbf{Q}^M, \bar{\mathbf{x}}^M\right) &\ge \mathbb{R}_{\min}^M, \quad \forall U_i \in \mathcal{U}_0, \\
Q_{0,i}^k &\ge Q_{0,i+1}^k, \quad \forall i = 1, \ldots, |\mathcal{U}_0| - 1, \forall SC_k \in \mathcal{SC}, \\
\sum_{U_i \in \mathcal{U}_0} \sum_{SC_k \in \mathcal{SC}} \bar{x}_{0,i}^k 2^{Q_{0,i}^k} + E_{C,0} &\le \mathcal{E}_0, \\
0 \le 2^{Q_{0,i}^k} &\le \bar{x}_{0,i}^k E^{\max}, \quad \forall SC_k \in \mathcal{SC}, \forall U_i \in \mathcal{U}_0, \\
\pi_k &\ge 0, \quad \forall SC_k \in \mathcal{SC}, \\
\rho_{0,i} &\ge 0, \quad \forall U_i \in \mathcal{U}_0, \\
\upsilon_{0,i}^k &\ge 0, \quad \forall i = 1, \ldots, |\mathcal{U}_0| - 1, \forall SC_k \in \mathcal{SC}, \\
\varsigma &\ge 0, \\
\omega_{0,i}^k, \varpi_{0,i}^k &\ge 0, \quad \forall SC_k \in \mathcal{SC}, \forall U_i \in \mathcal{U}_0. \qquad \text{(E.4)}
\end{aligned}
$$

$$
\frac{\partial \overline{\boldsymbol{GEE}}\left(\mathbf{Q}^M, \bar{\mathbf{x}}^M\right)}{\partial Q_{0,i}^k} = \frac{1}{\bar{E}_T\left(\mathbf{Q}^M, \bar{\mathbf{x}}^M\right)} \left(\frac{\partial \bar{R}_T\left(\mathbf{Q}^M, \bar{\mathbf{x}}^M\right)}{\partial Q_{0,i}^k} - \overline{\boldsymbol{GEE}}\left(\mathbf{Q}^M, \bar{\mathbf{x}}^M\right) \frac{\partial \bar{E}_T\left(\mathbf{Q}^M, \bar{\mathbf{x}}^M\right)}{\partial Q_{0,i}^k} \right) \qquad \text{(E.5)}
$$

$$\frac{\partial \boldsymbol{GEE}\left(\mathbf{Q}^M,\bar{\mathbf{x}}^M\right)}{\partial Q_{0,i}^k}-\ln(2)\sum_{SC_k\in\mathcal{SC}}\pi_k\sum_{U_i\in\mathcal{U}_0}\bar{x}_{0,i}^k 2^{Q_{0,i}^k}+\frac{\partial}{\partial Q_{0,i}^k}\sum_{U_i\in\mathcal{U}_0}\rho_{0,i}\left(R_{0,i}\left(\mathbf{Q}^M,\bar{\mathbf{x}}^M\right)-\mathbb{R}_{\min}^M\right)$$
$$+\frac{\partial}{\partial Q_{0,i}^k}\sum_{i=1}^{|\mathcal{U}_0|-1}\sum_{SC_k\in\mathcal{SC}}\upsilon_{0,i}^k\left(Q_{0,i}^k-Q_{0,i+1}^k\right)-\ln(2)\left(\varsigma\sum_{U_i\in\mathcal{U}_0}\sum_{SC_k\in\mathcal{SC}}\bar{x}_{0,i}^k 2^{Q_{0,i}^k}\right)$$
$$-\ln(2)\sum_{SC_k\in\mathcal{SC}}\sum_{U_i\in\mathcal{U}_0}\omega_{0,i}^k 2^{Q_{0,i}^k}+\ln(2)\sum_{SC_k\in\mathcal{SC}}\sum_{U_i\in\mathcal{U}_0}\varpi_{0,i}^k 2^{Q_{0,i}^k}=0. \tag{E.7}$$

$$\frac{\partial \boldsymbol{GEE}\left(\mathbf{Q}^M,\bar{\mathbf{x}}^M\right)}{\partial Q_{0,i}^k}=\frac{1}{E_T\left(\mathbf{Q}^M,\bar{\mathbf{x}}^M\right)}\left(\frac{\partial R_T\left(\mathbf{Q}^M,\bar{\mathbf{x}}^M\right)}{\partial Q_{0,i}^k}-\boldsymbol{GEE}\left(\mathbf{Q}^M,\bar{\mathbf{x}}^M\right)\frac{\partial E_T\left(\mathbf{Q}^M,\bar{\mathbf{x}}^M\right)}{\partial Q_{0,i}^k}\right) \tag{E.8}$$

where $\bar{\mathcal{I}}_{0,j}^k$ is the transformed intra-cell interference term. On the other hand, the first-order optimality conditions for the $\boldsymbol{GEE}\left(\mathbf{E},\bar{\mathbf{x}}^M\right)$ of problem **GEE-PA-Stage-1** must be verified in the $\mathbf{Q}^M$-space (i.e. by setting $\mathbf{E}^M=2^{\mathbf{Q}^M}$) and subject to constraints (19a)—(19e). Hence, $\frac{\partial \boldsymbol{GEE}\left(\mathbf{Q}^M,\bar{\mathbf{x}}^M\right)}{\partial Q_{0,i}^k}$ is obtained as given in (E.7)[20], as shown at the top of this page, where $\frac{\partial \boldsymbol{GEE}\left(\mathbf{Q}^M,\bar{\mathbf{x}}^M\right)}{\partial Q_{0,i}^k}$ is given in (E.8), as shown at the top of this page, and $\frac{\partial E_T\left(\mathbf{Q}^M,\bar{\mathbf{x}}^M\right)}{\partial Q_{0,i}^k}=\ln(2)\bar{x}_{0,i}^k 2^{Q_{0,i}^k}$. Moreover,

$$\frac{\partial R_T\left(\mathbf{Q}^M,\bar{\mathbf{x}}^M\right)}{\partial Q_{0,i}^k}=\frac{\bar{\gamma}_{0,i}^k}{\bar{\gamma}_{0,i}^k+1}-\sum_{j<i}\frac{\bar{\gamma}_{0,j}^k}{\bar{\gamma}_{0,j}^k+1}\frac{|h_{0,j}^k|^2}{\bar{\mathcal{I}}_{0,j}^k+N_0}\bar{x}_{0,i}^k 2^{Q_{0,i}^k}, \tag{E.9}$$

where

$$\bar{\gamma}_{0,j}^k=\frac{|h_{0,i}^k|^2\bar{x}_{0,i}^k 2^{Q_{0,i}^k}}{\bar{\mathcal{I}}_{0,i}^k+N_0}. \tag{E.10}$$

By comparing (E.6) and (E.9), it is evident that $\alpha_{0,i}^k=\frac{\bar{\gamma}_{0,i}^k}{\bar{\gamma}_{0,i}^k+1}$, $\forall U_i\in\mathcal{U}_0$, as per (23). Also, based on (24), $\beta_{0,i}^k=\log_2\left(1+\bar{\gamma}_{0,i}^k\right)-\alpha_{0,i}^k\log_2\left(\bar{\gamma}_{0,i}^k\right)$, $\forall U_i\in\mathcal{U}_0$. Since $E_T\left(\mathbf{Q}^M,\bar{\mathbf{x}}^M\right)=\bar{E}_T\left(\mathbf{Q}^M,\bar{\mathbf{x}}^M\right)$ (and hence $\frac{\partial E_T\left(\mathbf{Q}^M,\bar{\mathbf{x}}^M\right)}{\partial Q_{0,i}^k}=\frac{\partial \bar{E}_T\left(\mathbf{Q}^M,\bar{\mathbf{x}}^M\right)}{\partial Q_{0,i}^k}$), and upon convergence of **Algorithm 3**, $\bar{R}_{0,i}\left(\mathbf{Q}^M,\bar{\mathbf{x}}^M\right)\to R_{0,i}\left(\mathbf{Q}^M,\bar{\mathbf{x}}^M\right)$, and the bound in (22) becomes tight (i.e. an equality). Consequently, (E.3) and (E.7) become identical, and so are (E.4) and (E.8) (i.e. the same KKT conditions apply to problems **R-GEE-PA-Stage-1** and **GEE-PA-Stage-1** [32]). Hence, by iteratively updating the values of $\alpha_{0,i}^{k,(l)}$ and $\beta_{0,i}^{k,(l)}$ (i.e. tightening the lower-bound), the solution $\bar{\mathbf{E}}^M=2^{\bar{\mathbf{Q}}^M}$ of problem **GEE-PA-Stage-1**—that satisfies the KKT conditions—is obtained. ■

[20]The KKT conditions are necessary first-order conditions for the maximization of problem **GEE-PA-Stage-1** [32], where Slater's constraint qualification also holds [38].

APPENDIX F
LEMMA 6

Proof: This is a direct result of the finite number of subcarriers that can be swaped for each user pair. ■

APPENDIX G
LEMMA 7

Proof: Note that there are $\binom{|\mathcal{SC}|}{2}=\frac{1}{2}\left(|\mathcal{SC}|^2-|\mathcal{SC}|\right)$ subcarrier pairs, where $|\mathcal{SC}|=K$. Thus, the worst-case complexity is of order $\mathcal{O}\left(K^2\right)$ per user pair. ■

APPENDIX H
LEMMA 8

Proof: The proof of **Lemma 8** is two-fold. First, one must show that the resulting matching $\mathbf{x}^*$ is two-sided exchange-stable, and second, show that the resulting solution $(\mathbf{E}^*,\mathbf{x}^*)$ satisfies the KKT conditions. Now, in **Stage 2** of **Algorithm 5**, the swap matching algorithm (i.e. **Algorithm 4**) is repeatedly executed to eliminate any swap-blocking pairs. According to **Definition 13**, a swap-blocking pair is eliminated iff the rate of at least one user strictly improves, which must also strictly improve the network GEE, since the network total energy consumption remains fixed, as per **Remark 18**. Thus, by repeatedly eliminating swap-blocking pairs, and strictly monotonically improving (and optimizing) the network GEE, all swap-blocking pairs are eliminated, yielding a two-sided exchange-stable matching solution $\mathbf{x}^*$ in a finite number of iterations. On the other hand, in **Stage 1**, problem **GEE-PA-Stage-1** satisfies the KKT conditions, as per **Lemma 5**. Similarly, problem **GEE-PA-Stage-2** is optimally solved while satisfying the KKT conditions, as per **Proposition 2**. Hence, the obtained optimal solution $(\mathbf{E}^*,\mathbf{x}^*)$ of **Algorithm 5** also satisfies KKT conditions. ■

REFERENCES

[1] A. Damnjanovic, J. Montojo, Y. Wei, T. Ji, T. Luo, M. Vajapeyam, T. Yoo, O. Song, and D. Malladi, "A survey on 3GPP heterogeneous networks," *IEEE Wireless Commun.*, vol. 18, no. 3, pp. 10–21, Jun. 2011.

[2] R. Q. Hu and Y. Qian, "An energy efficient and spectrum efficient wireless heterogeneous network framework for 5G systems," *IEEE Commun. Mag.*, vol. 52, no. 5, pp. 94–101, May 2014.

[3] Y. Liu, Z. Qin, M. Elkashlan, Z. Ding, A. Nallanathan, and L. Hanzo, "Nonorthogonal multiple access for 5G and beyond," *Proc. IEEE*, vol. 105, no. 12, pp. 2347–2381, Dec. 2017.

[4] L. Dai, B. Wang, Y. Yuan, S. Han, C.-L. I, and Z. Wang, "Non-orthogonal multiple access for 5G: Solutions, challenges, opportunities, and future research trends," *IEEE Comms. Mag.*, vol. 53, no. 9, pp. 74–81, Sep. 2015.
[5] Y. Chen, S. Zhang, S. Xu, and G. Y. Li, "Fundamental trade-offs on green wireless networks," *IEEE Comms. Mag.*, vol. 49, no. 6, pp. 30–37, Jun. 2011.
[6] M. Vaezi, Z. Ding, and H. V. Poor, *Multiple Access Techniques for 5G Wireless Networks and Beyond*. Basel, Switzerland: Springer, 2019. [Online]. Available: https://www.springer.com/gp/book/9783319920894
[7] M. W. Baidas and E. A. Alsusa, "Power allocation, relay selection and energy cooperation strategies in energy harvesting cooperative wireless networks," *Wireless Commun. Mobile Comput.*, vol. 16, no. 14, pp. 2065–2082, Oct. 2016.
[8] S. Zhang, N. Zhang, G. Kang, and Z. Liu, "Energy and spectrum efficient power allocation with NOMA in downlink HetNets," *Phys. Commun.*, vol. 31, pp. 121–132, Dec. 2018.
[9] D. Ni, L. Hao, Q. T. Tran, and X. Qian, "Power allocation for downlink NOMA heterogeneous networks," *IEEE Access*, vol. 6, pp. 26742–26752, 2018.
[10] M. Moltafet, P. Azmi, N. Mokari, M. R. Javan, and A. Mokdad, "Optimal and fair energy efficient resource allocation for energy harvesting-enabled-PD-NOMA-based HetNets," *IEEE Trans. Wireless Commun.*, vol. 17, no. 3, pp. 2054–2067, Mar. 2018.
[11] A. Celik, M.-C. Tsai, R. M. Radaydeh, F. S. Al-Qahtani, and M.-S. Alouini, "Distributed user clustering and resource allocation for imperfect NOMA in heterogeneous networks," *IEEE Trans. Commun.*, vol. 67, no. 10, pp. 7211–7227, Oct. 2019, doi: 10.1109/TCOMM.2019.2927561.
[12] B. Xu, Y. Chen, J. R. Carrión, and T. Zhang, "Resource allocation in energy-cooperation enabled two-tier NOMA HetNets toward green 5G," *IEEE J. Sel. Areas Commun.*, vol. 35, no. 12, pp. 2758–2770, Dec. 2017.
[13] F. Fang, J. Cheng, and Z. Ding, "Joint energy efficient subchannel and power optimization for a downlink NOMA heterogeneous network," *IEEE Trans. Veh. Technol.*, vol. 68, no. 2, pp. 1351–1364, Feb. 2019.
[14] L. Salaun, C. S. Chen, and M. Coupechoux, "Optimal joint subcarrier and power allocation in NOMA is strongly NP-hard," in *Proc. IEEE Int. Conf. Commun. (ICC)*, May 2018, pp. 1–7.
[15] D. Gale and L. S. Shapley, "College admissions and the stability of marriage," *Amer. Math. Monthly*, vol. 69, no. 1, pp. 9–15, Jan. 1962.
[16] E. Bodine-Baron, C. Lee, A. Chong, B. Hassibi, and A. Wierman, "Peer effects and stability in matching markets," in *Algorithmic Game Theory* (Lecture Notes in Computer Science), vol. 6982. Berlin, Germany: Springer, 2011, pp. 117–129. [Online]. Available: https://link.springer.com/chapter/10.1007/978-3-642-24829-0_12
[17] A. Zappone, E. Björnson, L. Sanguinetti, and E. Jorswieck, "Globally optimal energy-efficient power control and receiver design in wireless networks," *IEEE Trans. Signal Process.*, vol. 65, no. 11, pp. 2844–2859, Jun. 2017.
[18] F. Echenique and J. Oviedou, "A theory of stability in many-to-many matching markets," *Theor. Econ.*, vol. 1, no. 2, pp. 233–273, Jun. 2006.
[19] P. Eirinakis, D. Magos, I. Mourtos, and P. Miliotis, "Finding a minimum-regret many-to-many stable matching," *Optimization*, vol. 62, no. 8, pp. 1007–1018, 2013.
[20] A. E. Roth, "Deferred acceptance algorithms: History, theory, practice, and open questions," *Int. J. Game Theory*, vol. 36, pp. 537–569, Mar. 2008.
[21] Z. Jiao and G. Tian, "The blocking lemma and strategy-proofness in many-to-many matchings," *Games Econ. Behav.*, vol. 102, pp. 44–55, Mar. 2017.
[22] R. Martínez, J. Massó, A. Neme, and J. Oviedo, "An algorithm to compute the full set of many-to-many stable matchings," *Math. Social Sci.*, vol. 47, pp. 187–210, Mar. 2004.
[23] Z. Jiao and G. Tian, "The stability of many-to-many matching with max–min preferences," *Econ. Lett.*, vol. 192, pp. 52–56, Apr. 2015.
[24] A. E. Roth, "Stability and polarization of interests in job matching," *Econometrica*, vol. 52, pp. 47–57, Jan. 1984.
[25] M. Baïou and M. Balinski, "Many-to-many matching: Stable polyandrous polygamy (or polygamous polyandry)," *Discrete Appl. Math.*, vol. 101, pp. 1–12, Apr. 2000.
[26] A. Zappone and E. Jorswieck, "Energy efficiency in wireless networks via fractional programming theory," *Found. Trends Commun. Inf. Theory*, vol. 11, nos. 3–4, pp. 185–399, 2014.
[27] J. Papandriopoulos and J. S. Evans, "Low-complexity distributed algorithms for spectrum balancing in multi-user DSL networks," in *Proc. IEEE Int. Conf. Commun.*, Jun. 2006, pp. 3270–3275.
[28] S. Boyd and L. Vandenberghe, *Convex Optimization*. Cambridge, U.K.: Cambridge Univ. Press, 2003.
[29] J.-P. Crouzeix and J. A. Ferland, "Algorithms for generalized fractional programming," *Math. Program.*, vol. 52, no. 1, pp. 191–207, May 1991.
[30] J.-P. Crouzeix, J. A. Ferland, and H. Van Nguyen, "Revisiting Dinkelbach-type algorithms for generalized fractional programs," *OPSEARCH*, vol. 45, no. 2, pp. 97–110, Jun. 2008.
[31] W. Dinkelbach, "On nonlinear fractional programming," *Manage. Sci.*, vol. 13, no. 7, pp. 492–498, Mar. 1967.
[32] L. Venturino, A. Zappoine, C. Risi, and S. Buzzi, "Energy-efficient scheduling and power allocation in downlink OFDMA networks with base station coordination," *IEEE Trans. Wireless Commun.*, vol. 14, no. 1, pp. 1–14, Jan. 2015.
[33] Q.-T. Vien, T. A. Le, B. Barn, and C. V. Phan, "Optimising energy efficiency of non-orthogonal multiple access for wireless backhaul in heterogeneous cloud radio access network," *IET Commun.*, vol. 10, no. 18, pp. 2516–2524, 2016.
[34] H. Q. Tran, P. Q. Truong, C. V. Phan, and Q.-T. Vien, "On the energy efficiency of NOMA for wireless backhaul in multi-tier heterogeneous CRAN," in *Proc. IEEE Int. Conf. Recent Adv. Signal Process. (SigTelCom)*, Jan. 2017, pp. 229–234. [Online]. Available: https://ieeexplore.ieee.org/document/7849827
[35] M. Schlueter, "MIDACO software performance on interplanetary trajectory benchmarks," *Adv. Space Res.*, vol. 54, no. 4, pp. 744–754, 2014.
[36] R. G. Ródenas, M. L. López, and D. Verastegui, "Extensions of Dinkelbach's algorithm for solving non-linear fractional programming problems," *Top*, vol. 7, no. 1, pp. 33–70, Jun. 1999.
[37] A. Zappone, L. Sanguinetti, G. Bacci, E. Jorswieck, and M. Debbah, "Energy-efficient power control: A look at 5G wireless technologies," *IEEE Trans. Signal Process.*, vol. 64, no. 7, pp. 1668–1683, Apr. 2016.
[38] M. Slater, "Lagrange multipliers revisited," in *Traces and Emergence of Nonlinear Programming*. Basel, Switzerland: Birkhäuser, 2014, pp. 293–306. [Online]. Available: https://link.springer.com/chapter/10.1007/978-3-0348-0439-4_14

MOHAMMED W. BAIDAS (M'05–SM'17) received the B.Eng. degree (Hons.) in communication systems engineering from The University of Manchester, Manchester, U.K., in 2005, the M.Sc. degree (Hons.) in wireless communications engineering from the University of Leeds, Leeds, U.K., in 2006, the M.S. degree in electrical engineering from the University of Maryland, College Park, MD, USA, in 2009, and the Ph.D. degree in electrical engineering from Virginia Tech, Blacksburg, VA, USA, in 2012. He was a Visiting Researcher with The University of Manchester, from 2015 to 2016 and from 2018 to 2019. He is currently an Associate Professor with the Department of Electrical Engineering, Kuwait University, Kuwait, where he has been on the faculty, since May 2012. He is also a Frequent Reviewer for several the IEEE journals and international journals and conferences, with over 50 publications. His research interests include resource allocation and management in cognitive radio systems, game theory, cooperative communications and networking, and green and energy-harvesting networks. He also serves as a Technical Program Committee Member for various the IEEE and international conferences. He was a recipient of the Outstanding Teaching Award of Kuwait University, from 2017 to 2018.

MUBARAK AL-MUBARAK (S'19) received the B.Sc. degree in electrical engineering from Kuwait University, Kuwait, in 2018. He is currently pursuing the M.S. degree with The Ohio State University, Columbus, OH, USA. His research interests include smart-grids, power system optimization, dynamic analysis, stability and control, grid resilience, and renewable integration.

EMAD ALSUSA (M'06–SM'07) received the Ph.D. degree in telecommunications from the University of Bath, Bath, U.K., in 2000. In 2000, he became a Postdoctoral Researcher with Edinburgh University, Edinburgh, U.K. In September 2003, he joined The University of Manchester, where he is currently a Reader with the School of Electrical and Electronic Engineering. He is also the U.K. Representative of the International Union of Radio Science (URSI). He has supervised over 30 Ph.D.s/PDRAs. He has authored or coauthored over 200 journals and refereed conference publications, mainly in top the IEEE TRANSACTIONS and conferences. His research interests include in the areas of wireless networks and signal processing with particular focus on future ultraefficient networks through the design of novel techniques for radio resource management, interference manipulation, secret key exchange, and energy neutrality. He was a recipient of number of awards, including the Best Paper Award in the IEEE PLC-2014 and the IEEE WCNC-2019. He has served as the Conference General Co/Chair for the IEEE OnlineGreenCom, in 2017, and Sustainability through ICT Summit, in 2019, as well as the TPC Symposia-Chair of several the IEEE conferences, including ICC 2015, VTC 2016, GISN 2016, PIMRC 2017, and GLOBECOM 2018.

MOHAMAD KHATTAR AWAD (S'02–M'09–SM'17) received the B.A.Sc. degree in electrical and computer engineering (communications option) from the University of Windsor, Windsor, ON, Canada, in 2004, and the M.A.Sc. and Ph.D. degrees in electrical and computer engineering from the University of Waterloo, Waterloo, ON, Canada, in 2006 and 2009, respectively. From 2004 to 2009, he was a Research Assistant with the Broadband Communications Research Group (BBCR), University of Waterloo. In 2009 to 2012, he was an Assistant Professor of electrical and computer engineering with the American University of Kuwait. Since 2012, he has been with Kuwait University, where he currently is an Associate Professor of computer engineering. His research interests include wireless and wired communications, software-defined networks resource allocation, wireless networks resource allocation, and acoustic vector-sensor signal processing. He received the Ontario Research & Development Challenge Fund Bell Scholarship, in 2008 and 2009, the University of Waterloo Graduate Scholarship in 2009, and the Fellowship Award from the Dartmouth College, Hanover, NH, USA, in 2011. In 2015 and 2017, he received the Kuwait University Teaching Excellence Award and the Best Young Researcher Award, respectively. He serves on the Editorial Board of the IEEE TRANSACTIONS ON GREEN COMMUNICATIONS AND NETWORKING (TGCN).